IVANE JAVAKHISHVILI TBILISI STATE UNIVERSITY

FORSCHUNGZENTRUM JÜLICH

Beam Polarimetry Studies for Spin-Filtering Experiment at COSY, Jülich

by

Zara Bagdasarian

Supervisors: Nodar Lomidze(TSU HEPI)

Mirian Tabidze(TSU HEPI)

Hans Ströher (FZJ)

Faculty of Exact and Natural Sciences

Fundamental Physics

Module of Atomic, Nuclear and Particle Physics

July 2012

IVANE JAVAKHISHVILI TBILISI STATE UNIVERSITY
FORSCHUNGZENTRUM JÜLICH

Abstract

Faculty of Exact and Natural Sciences
Fundamental Physics
Module of Atomic, Nuclear and Particle Physics

by Master's student

Zara Bagdasarian

The subject of the quark transverse spin distribution is at the frontier in understanding of the spin structure of the nucleon. The "golden channel" for a direct measurement of the so-called transversity distribution is Drell-Yan process $p\overline{p} \to l\bar{l}$ in double polarized proton-antiproton collision, which requires polarized antiprotons. The PAX Collaboration aims to solve this problem.

To date, so-called spin-filtering method in storage rings appears to be the only possible option to achieve polarization for antiprotons. As a first step of PAX, optimization of the polarization build-up in **proton** beams was performed at the Cooler Synchrotron (COSY), Forschungzentrum Jülich (Germany). COSY provides both polarized and unpolarized cooled proton beams, creating good conditions to study the spin-filtering principle and to test the equipment.

In this thesis emphasis will be made on beam polarization lifetime measurements. These data were taken in August 2011 prior to spin-filtering runs, using a 49.3 MeV polarized proton beam scattering from a deuterium cluster target. Since the expected polarization build-up at COSY is in the order of $10^{-2}h^{-1}$, it is important to study how rapidly the precious beam polarization decreases over time. The polarization was measured by means of the double-ratio method on detected deuterons, coming from pd elastic scattering. As the by-product, deuteron break-up events were extracted and analyzed to add to the experimental data set, necessary to fix important constraints for investigating the role of the three-nucleon forces via Chiral Perturbation Theory (χPT).

Acknowledgements

This work would have not been possible without the support and encouragement of many people, both from physics and non-physics domains. Hence, I would like to take this opportunity to express my sincere gratitude to all of them who have always been with me and for me.

First of all I want to thank my supervisor Dr. Hans Ströher for all his support starting from Georgian-German Conference held in Tbilisi in 2010. His invitations to visit Forschungzentrum Jülich in 2010 and 2011 helped me a lot to become familiar with research held at Nuclear Physics Institute (IKP). His continuous support throughout the duration of my stay and rich advices helped me to improve my thesis, as well as power point presentation.

I wish to sincerely thank my supervisor, Dr. Nodar Lomidze, for introducing me to analysis methods both in Juelich and Tbilisi. His introductory lectures to kinematics gave me insight into processes, I was analyzing. I'm sincerely grateful to him for teaching me how to doubt acquired knowledge and results and how to come back to what is thought to be understood and how to rethink it one more time. He has always given me an exemplary guidance to develop the necessary skills and the way to cultivate the ability to think independently as a graduate student.

I want to thank Dr. Mirian Tabidze for his help and willingness to answer my questions both during my visist in Juelich and prior to that in Tbilisi. He was lecturing me one semester prior to start of my work on Master's thesis introductory course to Statistics Data Analysis. The skills of working in ROOT I acquired in this course were very helpful for my master thesis assignments.

I also want to emphasize that part of this course's laboratory sessions were held by David Mchedlishvili, who has always given very precise and valuable advices on code writing as well as operational system and software installations.

I am also indebted to David Chiladze, who helped me a lot by reviewing parts of my thesis and my presentation for the defense. He also gave me a number of valuable advices at different stages of my work, for which I'm very grateful.

I owe a debt of gratitude to Dr. Andro Katcharava for all the guidance, I received from him during last 2 years, for arranging all the visits, and also organizing Georgian-German Workshops and meetings in Tbilisi. I want to thank him and his lovely family for being the core of Tbilisi-Juelich cooperation, and for being the great support for everybody who comes from Georgia to Juelich.

I also want to thank the whole PAX collaboration for this successful experiment and the opportunity for my thesis research. I'm very grateful for the opportunity to meet all these wonderful people and their benevolence and willingness to answer my questions. I also want to thank all of my friends I met in Jülich for the unforgettable time I spent here. I really enjoyed this 6-month stay and I really hope to continue working on my PhD in the same wonderful environment.

Finally, and most importantly, I would like to thank my parents, whose constant love and support cannot be matched with any word. They taught me that knowledge is the best treasure, you can gather during your whole life, and they showed me by their own example how it is to do everything with great love and passion. I'm infinitely grateful to them for having the greatest effect on the formation of my personality, always giving me the greatest lessons and great encouragement, and at the same time letting me take responsibility for my decisions and grow into an independent person that I am now. I admire and love them dearly, and dedicating this thesis to them is the smallest thing I can do.

I also want to thank my sister and her lovely family, as well as my other relatives for being very supportive and proud of me, encouraging me to achieve more. I would like to justify the hopes pinned on me by my family and teachers, to make my small contribution to the development of science and to be a contributing member of my country, and to society in general. I think my thesis allowed me to do just that.

To my wonderful parents,
Luiza and Amik

Contents

Abbreviations

PAX	**P**olarized **A**ntiproton e**X**periment
QCD	**Q**uantum **C**hromo**D**ynamics
QED	**Q**uantum **E**lectro**D**ynamics
DIS	**D**eep **I**nelastic **S**cattering
STT	**S**ilicon **T**racking **T**elescope
COSY	**CO**oler **SY**nchroton
SLAC	National Accelerator Laboratory, originally named **S**tanford **L**inear **A**ccelerator **C**
J-Lab	Jefferson Lab: Thomas Jefferson National Accelerator Facility
PDF	**P**arton **D**istribution **F**unction
EMS	**E**uropian **M**uon **C**ollaboration
PID	**P**article **ID**entification parameter
FILTEX	**FILT**ering **EX**periment
TSR	**T**est **S**torage **R**ing in Heidelberg
ABS	**A**tomic **B**eam **S**ource
PIT	**P**olarized **I**nternal **T**arget
BRP	**B**reit **R**abi **P**olarimeter
TGA	**T**arget **G**as **A**nalyzer
HESR	**H**igh **E**nergy **S**torage **R**ing
χ**PT**	**Chi**ral **P**erturbation **T**heory

Physical Constants

Speed of Light c	=	$2.997\ 924\ 58 \times 10^8$ ms$^{-\mathrm{S}}$
Mass of Proton	=	0.938272 GeV/c^2
Mass of Neutron	=	0.93957 GeV/c^2
Mass of Deuteron	=	1.875613 GeV/c^2
Fine Structure Constant α	=	1/137.035999074

List of Figures

Chapter 1

Introduction

What is the world made of? This is the question physicists and non-physicists attempt to answer. One can provide beautiful answers to this question on different scales. One of which is the scale of nucleons consisting from quarks that is described below.
Historically, it was expected that spin $\frac{1}{2}$ of the proton is simply the sum of two parallel and one antiparallel spin-1/2 quarks adding to $s = 1/2$. However, the real picture of proton structure is much more complicated: the three quarks that give a nucleon its identity, the valence quarks, swim in a "sea" of virtual quarks and antiquarks that are constantly popping in and out of the vacuum. Moreover, gluons float about inside nucleons, holding the quarks together. All of these contribute to the nucleon's spin.

This dynamic structure of the nucleon is described in three quark distribution functions: the momentum distribution, which is very well known; helicity, which is well investigated at RHIC [1]; and transversity, that has not yet been directly measured. The transversity represents the difference of probabilities to find the quark inside the transversely polarized proton with its spin parallel or antiparallel to that of proton. The transversity distribution is directly accessible in Drell-Yan process, which is lepton-antilepton production from quark-antiquark annihilation. In principle, Drell-Yan is possible in transversely polarized proton-proton scattering, as a quark of one proton can interact with the antiquark sea of the other

proton. Unfortunately, transversity is not experimentally measurable under such conditions. In order to directly measure transversity, one needs a Drell-Yan process with transversely polarized protons and **antiprotons**. In this case, a valence quark of the proton annihilates with the valence antiquark of the antiproton. The Polarized Antiproton EXperiments (PAX) collaboration aims to perform this direct measurement at the High Energy Storage Ring (HESR) of the Facility for Antiproton and Ion Research (FAIR) in Darmstadt, Germany. However, methods that are based on Stern-Gerlach separation, developed to provide polarized proton beams via dedicated sources, are not suitable for antiprotons. The PAX collaboration intends to polarize antiprotons via the spin-filtering method, which was already tested for the protons at FILTEX experiment [2].

1.1 PAX at COSY

Spin 1/2 particles have two possible spin projections. Polarizing a beam of such particles could be accomplished by identifying and selectively discarding the particles in one of the two states. So-called spin-filtering is based on spin dependence of nuclear interactions. An unpolarized beam is stored in dedicated ring with a polarized internal target. The latter acts as "filter" for the unpolarized beam, since it is more "transparent" to one spin state of the particles than to the other. As the beam continuously passes through the target, one spin direction is depleted more than the other and the beam becomes increasingly polarized. As a first step in this research spin-filtering experiment in **proton** beams was performed at the Cooler Synchrotron (COSY) Jülich [3]. The purposes of this study were to commission and test the experimental hardware and develop dedicated procedures for the analysis.

1.2 Aims of the Thesis

1.2.1 Beam Polarization Lifetime

One of the important factors to be studied for spin-filtering is the beam polarization lifetime. A strong-focusing synchrotron like COSY has two different types of depolarizing resonances: 1) imperfection resonances, caused by magnetic field errors and misalignments of the magnets and 2) intrinsic resonances excited by horizontal fields due to the vertical focusing. Intrinsic resonances arise when there is simple relation between the spin tune and the vertical betatron tune. Depolarizing resonances may also arise due to a simple relation between spin tune and orbit or the synchrotron frequency. Here, spin tune is the net precession angle of the particle's magnetic moment during one turn in the machine. To quantify these effects, a dedicated measurement of the polarization lifetime with polarized beam was performed.

By comparing the polarization measured at the beginning of the cycle and after storing the beam for 5000s, one can deduce the beam polarization lifetime and understand its effect on the polarization build-up during the spin-filtering process. The polarimetry is performed via the double-ratio method for proton deuteron elastic scattering.

1.2.2 Study of Breakup Reactions

One of the by-products of this study is a breakup reaction, which can be very useful to test the predictive power of CHiral Perturbation Theory (χPT) [4]. The main goal of investigation is to provide data that can put constraints on chiral perturbation theory, particularly relevant to the effects of three-nucleon forces, which are implemented in the calculations to third order. Comparison between experiment and theory can be performed by the sampling method, developed specifically for the complex analysis of three-particle final states [5].

χPT is applied to the effective potential, defined as the sum of all possible irreducible diagrams. At present, the two-nucleon force is worked out and applied up to next-to-next-to-next-to-leading order (N^3LO) in the chiral expansion. It yields an accurate description of two-nucleon observables at low energy. Systems with three and more nucleons have so far only been analyzed up to next-to-next-to-leading order N^2LO. At this order one encounters the first non-vanishing contributions from the chiral three-nucleon force. There are few or no measurements between proton beam energies of 30 and 50 MeV; however, these energies are already large enough to possibly see significant effects due to three-nucleon forces and, at the same time, low enough to allow theoretical predictions based on chiral effective field theory. That is why data collected at the 49.3 MeV beam energy can be of use to study three nucleon continuum in proton deuteron breakup reaction.

1.3 Outline of the Thesis

This thesis will present a review of proton structure and explain the need for a transversity measurement in polarized proton antiproton collisions. Essentials of possible polarization build-up principle with antiproton beam in a storage ring will be also discussed, followed by the description of the COSY facility and ANKE detector set-up. The cycles, performed during beam time from August to October of 2011 will then be presented with the emphasis on runs dedicated to a beam polarization lifetime measurement. Afterwards, a detailed description of the analysis of these data will be given. The objectives of work are the measurement of polarization lifetime in the COSY ring and the study of deuteron breakup analyzing power

Chapter 2

Proton Structure

2.1 What is the World Made of?

One can give different answers to that question. For a biologist, the world is made of living organisms, for a chemist the world is made of molecules formed from atoms. The physicist will start to talk about atoms, and then proceed to talk about the protons, neutrons and electrons that make up an atom.

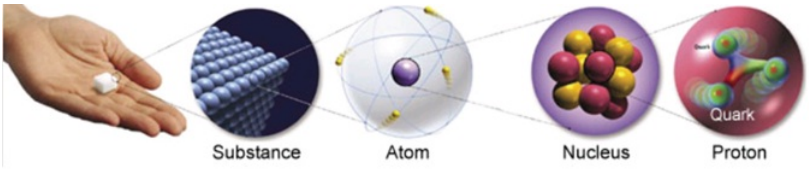

FIGURE 2.1: The progression of structure within structure of the familiar matter we see around us

We want to know: what are the fundamental, indivisible building blocks, which all the matter in the universe is made of? A series of important experimental discoveries changed our perceptions about the structure of the matter several times during the last century. The current status of our understanding can be displayed in the sequence: molecules $\rightarrow$ atoms $\rightarrow$ electrons and nuclei $\rightarrow$ nucleons $\rightarrow$ quarks.

The proton, neutron and electron are the basic building blocks of atomic matter. The proton was discovered in 1920 by Rutherford as the hydrogen nucleus, and was

believed to be a point-like particle. After more than 90 years the proton, as well as the neutron, have been proven to be complex entities [6], but their composition is still not fully understood. Experimental results suggest that the nucleon internal structure is considerably more complicated than had been once believed. Historically, a picture that three quarks are statically bound inside the nucleon has been predominant, with each quark, carrying 1/3 of the proton's linear momentum. The composition of the nucleons is now described by valence quarks, surrounded by virtual "sea" quark-antiquark pairs and particles carrying the force that bind quarks, aka gluons. The multitude of gluons and sea quark-antiquark pairs, each carrying generally a small fraction of the proton's momentum, contribute a large summed momentum overall.

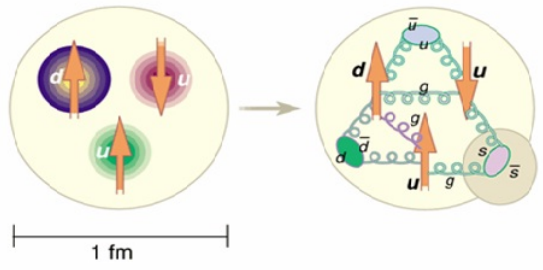

FIGURE 2.2: Nucleon Structure

2.2 Spin Crisis

In the naive model of the proton as simply three quarks of spin $\frac{1}{2}\hbar$ each, one might expect the proton's spin to be the straight forward sum of two parallel quark spins and one antiparallel. However, in the late 1980's it was discovered, that in fact only a small fraction of the proton's spin, only 14-23%, is carried by quarks [7] [8].This revelation, surprising at the time, came to be known as the "proton spin crisis". Gluon spins still don't add up to the total spin of the proton, so the spin crisis still remains nowadays and it requires dynamic structure of the nucleon. To describe it we need new quark distributions and fragmentation functions. Due to the fact that spatial rotations and Lorentz boosts do not commute, polarized proton structure must be considered separately for a proton with spin vector parallel

to or perpendicular to its momentum. This difference between the longitudinal and transverse spin structures adds further complexity to the discussed problem. Significant progress has been made in understanding the longitudinal spin structure (for example, at RHIC), while the transverse spin structure remains largely uninvestigated field.

2.3 Unpolarized Nucleon Structure

2.3.1 Magnetic Moments

The first evidence of proton substructure came from a measurement of its magnetic moment in 1933 by Estermann, Frisch, and Stern. It was found to be anomalously large and is now known to be approximately 2.79 times the Dirac magnetic moment, given by

$$\overrightarrow{\mu_p} = \frac{e}{Mc}\overrightarrow{S} \tag{2.1}$$

for a point-like spin 1/2 particle with the mass of proton. Similarly, the magnetic moment of the neutron was also found to be anomalous by Estermann and Stern in 1934. The magnetic moment of nucleons is nowadays understood in terms of its valence quark structures.

2.3.2 Form Factors

Charge and current distributions within the nucleon can be described by electromagnetic form factors, measured via elastic electron-proton scattering. Viewed in the particular reference frame, known as Breit frame ($\overrightarrow{p}_{fin} = -\overrightarrow{p}$), the form factors G_E and G_M are proportional to the Fourier transforms of the charge and magnetization distributions, respectively.

The cross-section for elastic electron-proton scattering can be expressed in terms of the form factors

$$\frac{d\sigma}{d\Omega}|_{lab} = \frac{\alpha^2}{4E^2 sin^4(\theta/2)} \frac{E'}{E} \left(\frac{G_E^2 + G_M^2}{1+\tau} cos^2\frac{\theta}{2} + 2\tau G_M^2 sin^2\frac{\theta}{2} \right) \tag{2.2}$$

where $\tau \equiv -q^2/4M^2$, q is the four-momentum transfer in the scattering, M is the proton mass, α is the fine structure constant, θ is the electron scattering angle in the laboratory frame, and E and E' are the incident and scattered electron energies. Proton electromagnetic form factor measurements have been performed, e.g. at Jefferson Lab [9] and show the sizes of charge and magnetization distributions.

2.3.2.1 Structure Functions

The nucleon structure functions describe the inelastic structure of the proton and neutron, probed principally via Deep Inelastic Scattering (DIS). The double differential cross section for electron-proton scattering can be expressed as

$$\frac{d\sigma}{dE' d\Omega}|_{lab} = \frac{4\alpha^2 E'^2}{q^4} \left(W_2(\nu, q^2) cos^2 + 2W_1(\nu, q^2) sin^2\frac{\theta}{2} \right) \tag{2.3}$$

in which q, α, θ, and E' are defined as in Eq. 2.2, $\nu = (p \cdot q)/M$ with p being the initial nucleon four-momentum, and W_1 and W_2 are the proton structure functions. There is similarity with the cross section for elastic electron-proton scattering, with the structure functions playing the role of the form factors. It is common to express the proton structure functions slightly differently, as

$$\begin{aligned} F_1 &= MW_1 \\ F_2 &= \nu W_2 \end{aligned} \tag{2.4}$$

F_1 and F_2 can be written as functions of $Q^2 = -q^2 > 0$ and the dimensionless variable $x = \frac{Q^2}{2p \cdot q}$ [10]. In 1969 Bjorken predicted that at large Q^2, scattering off the point-like subcomponents that were approximately free in the proton would lead to proton structure functions with no Q^2 dependence for a given value of

x [11]. In other words, assuming point-like constituents of the proton, inelastic electron-proton scattering could be viewed as elastic scattering of an electron off of a hard, point-like particle within the proton. The experiments performed at SLAC discovered the scaling behavior predicted by Bjorken [6]. The measured structure functions had very little explicit dependence on Q^2 and could, in fact, be written simply as functions of x. In 1969 Callan and Gross predicted that for spin 1/2 charged components within the nucleon, the scaling structure functions would be related as

$$F_2(x) = 2xF_1(x) \tag{2.5}$$

known as Callan-Gross relation [12]. It was experimentally confirmed at SLAC in the late 1970s, thus providing strong evidence for the spin $\frac{1}{2}$ nature of what are now known as quarks.

2.3.2.2 Parton Distribution Functions

Introduction of the quark-parton model (QPM) by Feynman in 1969 offered a relatively intuitive explanation of Bjorken scaling [13]. The virtual photon in DIS could be viewed as scattering elastically off a collection of hard partons within the proton; the DIS cross section is incoherent sum of the individual cross sections. As the proton momentum approaches infinity, x can be considered as the fraction of the proton's linear momentum carried by the parton. The size of the cross section for scattering off of a particular parton is proportional to the $q(x)$ probability of hitting a quark of flavor q carrying momentum fraction x of the proton. $q(x)$ is known as a parton distribution function (PDF). The scaling structure functions, $F_1(x)$ and $F_2(x)$ can then be viewed as representing the probability of scattering off of a parton within the proton carrying momentum fraction x.

2.3.3 QCD

The experimental and theoretical work in 1960's and 70's regarding hadronic interactions and structure led to the development of Quantum Chromo Dynamics

Theory (QCD), a thoery, which describes the behavior of the strong force. The central concept of QCD is the asymptotic freedom. While quarks are strongly bound at distance scales larger than a typical hadron radius ($r \approx 10^{-15}$ m), at short distances they behave as nearly free. QCD has successfully accounted for the strong interaction processes observed at high energy particle colliders, for example jet productions. Even with this success, QCD has not yet provided a complete explanation on the structure of hadrons. At this moment, experiment is the only way to extract information on non-perturbative confining effects in hadrons.

2.3.4 Perturbative QCD

Performing calculation in QCD presents a number of challenges that quantum electrodynamics (QED) calculations do not have. In QCD the force carriers are charged themselves; gluons carry color charge, whereas photons are electrically neutral. Contributions from higher-order Feynman scattering diagrams in QED, i.e. higher powers in electromagnetic coupling constant, $\alpha = 1/137$, representing additional lepton-photon vertices, quickly become negligibly small, due to the fact that α is much less than one. An analogous expansion in QCD is only possible in the range where the coupling, $\alpha_s(Q^2)$ is small, which is generally the case for processes involving a large momentum transfer. Perturbative QCD is the calculation technique used in this kinematic regime.

A hadron can be viewed as a a collection of free, massless partons with parallel momenta. The collinear factorization of the partons and hadrons implies that there is no transverse momentum of the partons in the proton with respect to the initial proton momentum, and no transverse momentum of the final-state hadron with respect to the scattered parton momentum. The factorization theorem was developed and proven over the course of the late 1970's to the mid-1980's [14] [15]. Along with factorization, there is the principle of universality, which states that PDF's and FF's are the same regardless of the scattering process involved. Universality implies the dominance at high momentum transfer of leading-twist (twist two) contributions, with interactions only between the two hard-scattering

partons. A higher-twist calculation takes into account the exchange of additional gluons between the hard-scattering partons and the nucleon remnants. It should be pointed out that the factorization theorem has not been proven generally for the case of non-collinear partons. It has so far only been proven for the Drell-Yan process [16]. Decades of comparison between experimental cross section measurements and QCD have provided a testing ground for the assumption of universality, and by now it is a well established and accepted principle. PDF's are not calculable in pQCD and are typically obtained from experiment, however in principle they are calculable using other theoretical techniques. Because of universality, PDF's and FF's can be measured in the environment which allows the most accurate determination and then utilized as input for pQCD.

2.3.5 Chiral Perturbation Theory

Chiral Perturbation Theory(χPT) is the effective field theory of QCD developed to study the properties of hadronic systems at low energies in a model-independent framework. It is based on the spontaneously broken chiral symmetry of QCD, providing a method to improve the results by considering higher orders in a perturbative expansion. The interaction with the gluons is the same for all flavours within QCD, the only difference between a u- and a d-quark, for instance, is that m_u differs from m_d. If the masses of the two lightest quarks were the same, QCD would have an exact isospin symmetry: invariance under rotations in the internal space spanned by the two lightest flavours. Disregarding the electromagnetic interaction, the splitting within these multiplets is due entirely to the difference between m_u and m_d. For isospin to represent an approximate symmetry, the difference m_u-m_d must be small and vice versa: if the difference is small, then QCD is approximately symmetric under the group SU(2) of isospin rotations. Small compared to what? QCD has an intrinsic scale, Λ_{QCD}, which is independent of the quark masses and carries the dimension of an energy. Expressing the quark masses in energy units, the condition for isospin to be an approximate symmetry can be written as $m_u - m_d << \Lambda_{QCD}$.

In the low-energy regime of QCD, the degrees of freedom are no longer quarks and gluons, but rather hadrons. This is a result of confinement. If one could "solve" the QCD partition function, (such that the degrees of freedom in the Lagrangian are replaced by hadrons) then one could extract information about low-energy physics. A low-energy effective theory with hadrons as the fundamental degrees of freedom is a possible solution. According to Steven Weinberg, an effective theory can be also useful for few nucleon sector, if one writes down all terms consistent with the symmetries of the parent theory. In general there are an infinite number of terms which meet this requirement. Therefore in order to make any physical predictions, one assigns the theory a power counting scheme which organizes terms by a pre-specified degree of importance which allows one to keep some terms and reject all others as higher-order corrections which can be safely neglected. In addition, unknown coupling constants, also called low-energy constants (LECs), are associated with terms in the Lagrangian that can be determined by fitting to experimental data or be derived from underlining theory.

2.4 Polarized Proton Structure

In the late 1980's the EMC (Europian Muon Collaboration) experiment at CERN discovered, that only approximately 13-16% of the proton's spin was due to the spin of the quarks. With so little coming from the total quark spin ($\delta\Sigma$) the remainder is expected to come from gluon spin contributions (δg) and the orbital angular momentum of both quarks and gluons (L_{g+q})

$$\frac{1}{2} = \frac{1}{2}(\delta\Sigma) + \delta g + L_{g+q} \tag{2.6}$$

2.4.1 Polarized Structure Functions

Similar to the already discussed unpolarized structure functions, spin-dependent structure functions can also be defined. The difference in cross sections for deep-inelastic scattering of leptons polarized antiparallel and parallel to the spin of the

target proton can be written as

$$\frac{d^2\sigma^{+-}}{dQ^2\nu} - \frac{d^2\sigma^{++}}{dQ^2\nu} = \frac{4\pi\alpha^2}{E^2Q^2}\left[M(E + E'cos\theta)G_1(\nu, Q^2) - Q^2G_2(\nu, Q^2)\right] \tag{2.7}$$

in which the kinematic variables are defined as in Eq. 2.2 and Eq. 2.3, while G_1 and G_2 represent polarized structure functions of the proton. In the Bjorken scaling limit of large Q^2 and ν, these structure functions depend only on x and can be given as in

$$\begin{aligned} g_1(x) &= M^2\nu G_1(\nu, Q^2) \\ g_2(x) &= M\nu^2 G_2(\nu, Q^2) \end{aligned} \tag{2.8}$$

$g_1(x)$ can be viewed as the difference in probability of scattering off of a parton carrying momentum fraction x of the proton with parton helicity antiparallel versus parallel to the proton spin.

The transverse spin structure of the proton cannot be determined from its longitudinal spin structure. Inelastic proton-proton or quark-proton scattering can be considered in terms of elastic quark-proton scattering. In the elastic scattering of two spin $\frac{1}{2}$ particles, there are three different possibilities for the initial and final-state helicities. The particles may start and end with the same helicity (++ →++) start and end with opposite helicities (+- →+-), or start with opposite helicities and change helicities in the scattering (+- → -+). Linear combinations of these three helicity configurations in the scattering can be formed, corresponding to the momentum(q), helicity (Δq), and transversity (δq) distribution functions given by:

q	(++ →++) + (+- →+-)
Δq	(++ →++) - (+- →+-)
δq	(+- → -+)

Transveristy is therefore a chiral-odd, or "helicity-flip", distribution. In a transverse basis, it represents the difference in probability of scattering off a quark with

parellel and antiparallel spin to the one of proton, within the transversely polarized proton. This interpretation is directly analogous to the meaning of helicity distribution in helicity basis.

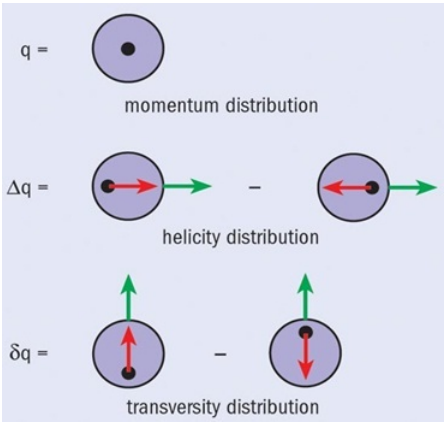

FIGURE 2.3: Polarized Parton Distributions

The only known relation that connects these three functions is the Soffer inequality [17]:

$$q(x) + \Delta q(x) \geq 2|\delta q(x)| \tag{2.9}$$

The quark transverse polarization does not mix with the gluon polarization because gluon carry out only longitudinal spin and there is no mechanism to flip the helicity of (spin-1) gluons in the scattering. That is the reason, why it is impossible to measure δq in Deep Inelastic Scattering (DIS). Direct measurement of transversity requires another chiral-odd partner. One possibility is to look for observables that represent the convolution of two transversity distributions, i.e. double transverse-spin asymmetries, A_{TT}, for example, in Drell-Yan production of lepton pairs in the collision of two hadrons.

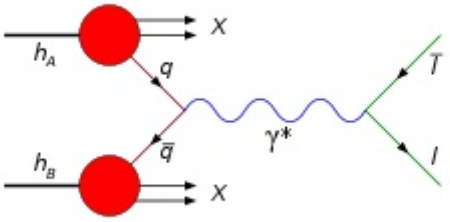

FIGURE 2.4: Feynman diagram for Drell-Yan Process

The golden channel to perform a self-sufficent measurement is the lepton pair production in double polarized Drell-Yann collisions of proton-antiproton $\bar{p}^{\uparrow}p^{\uparrow} \rightarrow l\bar{l}X$

$$A_{TT} = \frac{\sigma^{\uparrow\uparrow} - \sigma^{\uparrow\downarrow}}{\sigma^{\uparrow\uparrow} + \sigma^{\uparrow\downarrow}} = a_{TT} \frac{\Sigma_q e_q^2 \delta q(x_1, Q^2) \delta q(x_2, Q^2)}{\Sigma_q e_q^2 q(x_1, Q^2) q(x_2, Q^2)} \tag{2.10}$$

Here a_{TT} is double spin asymmetry in elementary QED process which is well known, and q indexes stand for quark flavor (u, d, s ..). In pp Drell-Yan A_{TT} is very small (for example at RHIC energies: $A_{TT}/a_{TT} \sim 1\%$) and practically is hard to be measured; also accessing x region is very restricted. In case of proton antiproton scattering, with both target and beam transversely polarized at PAX energies ($s \sim 30 - 50GeV$, $x_1 x_2 \sim 0.2 - 0.3$) $A_{TT}/a_{TT} \sim 0.2$, and it is large enough to be measured. Moreover accessed x region is also wide. Furthermore, there are other objectives, as the origin of dependence of the ratio of the magnetic and electric form factors on Q^2(observed at the J-Lab) requiring additional research to discriminate which model for the form factors is justified, specifically a measurement of magnetic and electric Form Factor relative phase in the time-like region.

In other words, we urge for polarized antiprotons, because the polarized antiproton-proton interactions can provide an access to a number of new fundamental physics observables, which can't be studied without transverse polarization. PAX at COSY is the first stage of Polarized Anti-proton eXperiment, the ultimate goal of which is to store an intense beam of polarized antiprotons. All the equipment and analysis approaches are tested on protons at COSY, Juelich. The appropriate anti-proton storage technique nowadays is available only in CERN at the Antiproton Decelerator (AD) Ring and that's where PAX experiment wants to test polarizing method on antiprotons. The PAX experiment could later become one of the cornerstones of the FAIR (Facility for Antiproton and Ion Research), Darmshtadt, Germany, which will be built and ready for use towards the end of the decade.

Chapter 3

Background Experiments and Theory

Realization of antiproton polarization, storing of polarized antiprotons and finally accomplishment of a double-polarized antiproton-proton collider can drastically change situation in our understanding of nucleon structure. But so far high luminosity experiments with polarized antiprotons have been impossible.

3.1 A Little Bit of History

Some 30 years ago there was no shortage of rough ideas on how antiproton polarization might be accomplished. However up to now, the only polarized antiprotons available for use were in a secondary beam facility at FermiLab in 1990s, which made use of decay of antihyperons, but they are produced with extremely low intensities.

Spin 1/2 particles have two possible spin projections. Polarizing a beam of such particles could be accomplished by identifying and selectively discarding the particles in one of the two states. The separation of the spin states could be accomplished via the interaction of the magnetic moments with external fields (known as Stern-Gerlach effect), or via the spin dependence of a nuclear reaction (known

as spin filtering). While there is doubt about the former scheme feasibility even in principle, the second method has actually been successfully experimentally tested. A spin 1/2 beam could also be polarized if particles in one spin state would be moved into the other state (by spin-flipping). Spin Flip is the method based on spin transfer between protons and electrons, and was expected to be used for antiprotons via interacting with positrons. Because of the protons' much larger masses, those scattering from electrons always stay within acceptance. That would have led to no beam loss. The advantage over the spin filter method is obvious, since the precious stored beam is conserved. However, this idea was recently subjected to the experimental test at COSY, and an upper limit for spin-flip cross section was established, that ruled out the prospect of using spin flip to polarize a stored beam [18].

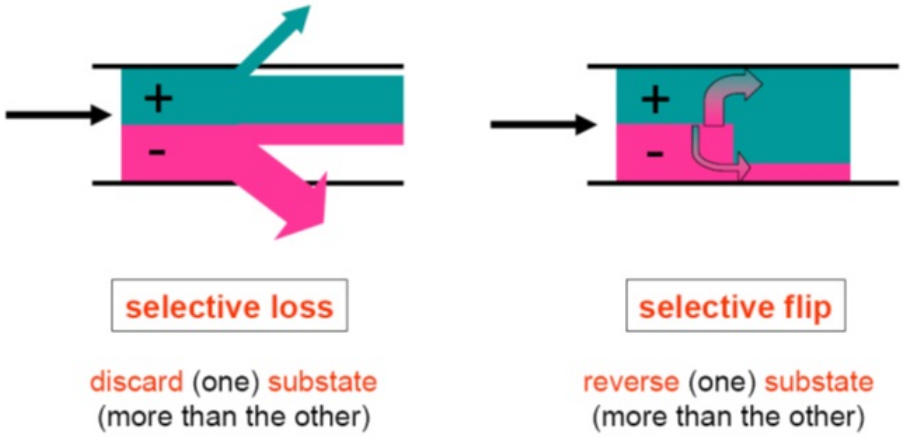

FIGURE 3.1: Spin Filtering and Spin Flip Working Principles

3.2 Spin-Filtering Working Principle

A polarized hydrogen or deuteron gas target is inserted in storage ring. The dipole-magnets of a cyclotron fix the stable polarization axis parallel or antiparallel to the magnetic fields. For a spin $\frac{1}{2}$ particle, like a proton or antiproton, two spin states "up"↑ and "down" ↓ are possible. N↑ (N↓) is the number of particles with

spin states "up"("down") and the beam polarization P is then defined by:

$$P = \frac{N\uparrow - N\downarrow}{N\uparrow + N\downarrow} \tag{3.1}$$

Since in general the total hadronic cross section is different for parallel and an-

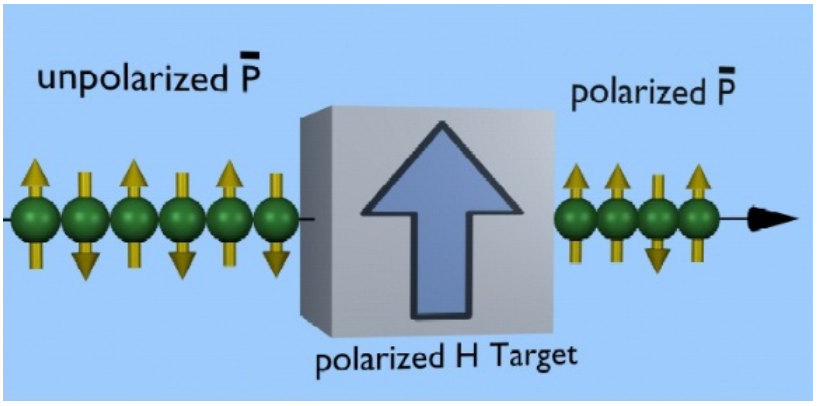

FIGURE 3.2: Spin Filtering Principle

tiparallel orientation of interacting particles, beam particles with spin direction parallel to the one of the target are depleted more than the others, leaving the circulating beam polarized, while the intensity of the beam decreases with the time. The total strong interaction cross section of the beam with the target is expressed as

$$\sigma_T = \sigma_0 + \sigma_1(\mathbf{P_B} \cdot \mathbf{Q_T}) + \sigma_\mathbf{2}(\mathbf{P_B} \cdot \mathbf{k})(\mathbf{Q_T} \cdot \mathbf{k}) \tag{3.2}$$

where $\mathbf{P_B}$ and $\mathbf{Q_T}$ are the beam and the target polarizations, σ_0 is the spin-independent part, while σ_1 and σ_2 are the spin-dependent parts of the cross section, describing the effect of the relative orientation of $\mathbf{P_B}$, $\mathbf{Q_T}$ and the beam direction, given by the unit vector $\mathbf{k}$.

Assuming $|\mathbf{P_B}| = |\mathbf{Q_T}| = \mathbf{1}$ the cross sections for the transverse and the longitudinal cases are

$$\begin{aligned} \sigma^{\perp}_{T\pm} &= \sigma_0 \pm \sigma_1 \\ \sigma^{||}_{T\pm} &= \sigma_0 \pm (\sigma_1 + \sigma_2) \end{aligned} \tag{3.3}$$

where the positive and negative sign applies respectively to the fraction of the beam whose spin is parallel and antiparallel to the spin of the target.

3.2.1 Polarization Build-up

If we neglect mechanisms other than interaction with the target, the intensity of the spin-up and spin-down particles in the stored beam each decrease exponentially, but with different time constants. In the absence of depolarization this leads to the resulting beam polarization build-up as a function of filter time t, that can be expressed as

$$P(t) = tanh(t/\tau_1) \tag{3.4}$$

where

$$\tau_1^{\perp} = \frac{1}{\sigma_1' Q_T d_T f} \tag{3.5}$$

$$\tau_1^{||} = \frac{1}{(\sigma_1' + \sigma_2') Q_T d_T f} \tag{3.6}$$

are the time constants that characterize the rates of polarization build up for transverse and longitudinal filtering respectively, where d_T is the target thickness in $atoms/cm^2$ and f is particles revolution frequency in the ring. The filtering cross sections σ_1' and σ_2' are closely related to the spin-dependent total cross-sections σ_1 and σ_2. The difference arises because protons (antiprotons) that scatter at a sufficiently small angle remain in the ring. Thus, while σ_1 and σ_2 are integrated in polar angle from 0 to 180°, σ_1' and σ_2' are only integrated from θ_{acc} to 180°.
In order to build up significant polarization, the beam has to pass through the target for times t of the order of τ_1. Meanwhile the intensity of the stored beam decreases with the time t according to

$$I_{\uparrow}(t) = \frac{I_0}{2} e^{-t/\tau_s} e^{(}t/\tau_1^{\perp}) \tag{3.7}$$

for part of beam with polarization up,

$$I_{\downarrow}(t) = \frac{I_0}{2} e^{-t/\tau_s} e^{(} - t/\tau_1^{\perp}) \tag{3.8}$$

for part of beam with polarization down, and therefore the intensity of the whole stored beam decreases with the time t according to

$$I(t) = I_0 e^{-t/\tau_s} cosh(t/\tau_1^{\perp}) \tag{3.9}$$

where τ_s is defined as

$$\tau_s = \frac{1}{\sigma_0 + \sigma_C} \tag{3.10}$$

It depends on σ_0, the spin-independent part of the nuclear total section, and σ_C, representing the loss of particles by small-angle Coulumb scattering either in the target or in the residual gas of the ring (hence the importance of residual gas pressure). σ_C is finite because particles scattered by sufficiently small-angle are within the ring acceptance and thus are retained; the limiting angle that is still accepted depends on the ion-optic properties of the ring (β function) at the target position. Straight section was chosen to minimize loss of particles, since Coulomb scattering attenuates the beam but doesn't contribute to the polarization build-up [2].

The goal while performing a spin-filtering is to reach as small as possible filter times and highest possible beam polarization. In order to reach the first goal especially the target density d_T has to be maximized and the experiment has to be carried out at an energy, where the spin-dependent cross section σ_1 is maximized. That's why we need only relatively low energies of the circulating beam because with increasing energy the strong interaction cross section decreases, leading to even slower polarization build-up. Conflicting with the aim to maximize the spin-dependent cross section σ_1 is the goal to minimize the Coulomb beam losses, therefore optimum beam energy is chosen. Nevertheless, the choice of the optimum energy for filtering doesn't preclude the use of the beam at higher or lower energies, because the stored beam can be accelerated or decelerated to the desired energy after filtering.

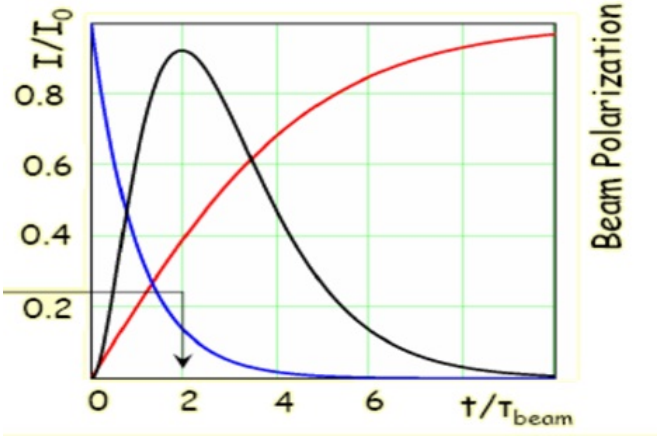

FIGURE 3.3: The blue line describes intensity decrease in beam lifetime units, The red line shows Beam Polarization build-up, and finally, figure of Merit function is shown in black line

Optimum time for polarization build-up is given by the maximum of figure of merit (Fig. 3.3)

$$FOM(t) = P(t)^2 I(t) \tag{3.11}$$

which is reached at t= 2 τ_b, where τ_b is the beam lifetime, thus the time,that it takes for intensity to decrease by e factor). The effects of depolarizing must be eliminated by suppressing the effect of imperfection resonances as well as for intrinsic resonances so we gain increased polarization lifetime. Further increase in beam time polarization can be expected if the beam lifetime is increased. Minimal lifetime for spin-filtering studies at COSY is 5000 s. During the beamtime in August-September 2011 the beam lifetime was in average 8000 seconds.
It is important to quantify depolarizing rate for the duration of spin-filtering, since it may reduce expected polarization build-up.

3.3 FILTEX experiment

Spin Filtering was first proposed by Csonka, and demonstrated by FILTEX experiment. In 1992 at the Test Storage Ring (TSR) in Heidelberg this method to polarize a stored beam was tested with a proton beam. The experimental setup of the spin filter experiment is displayed in Fig. 3.4. In this experiment a 23MeV

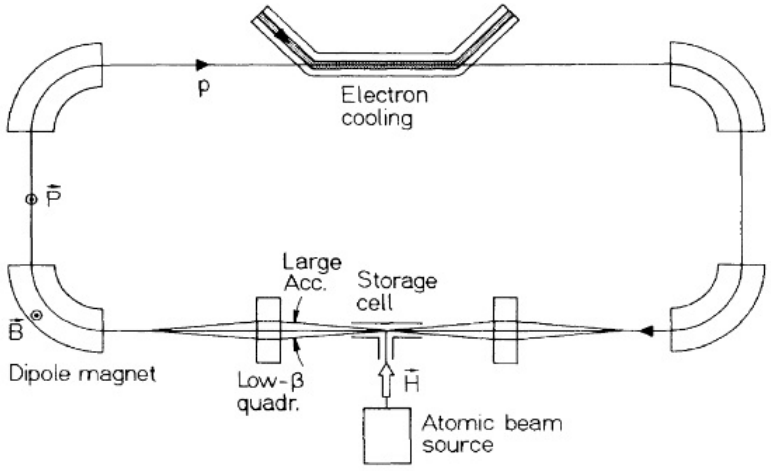

FIGURE 3.4: Test Storage Ring scheme with installations for the FILTEX Experiment

stored proton beam was passing through an internal, transversely polarized hydrogen gas target of a thickness of $d_t = (5.3 \pm 0.3) \cdot 10^{13} atoms/cm^2$.

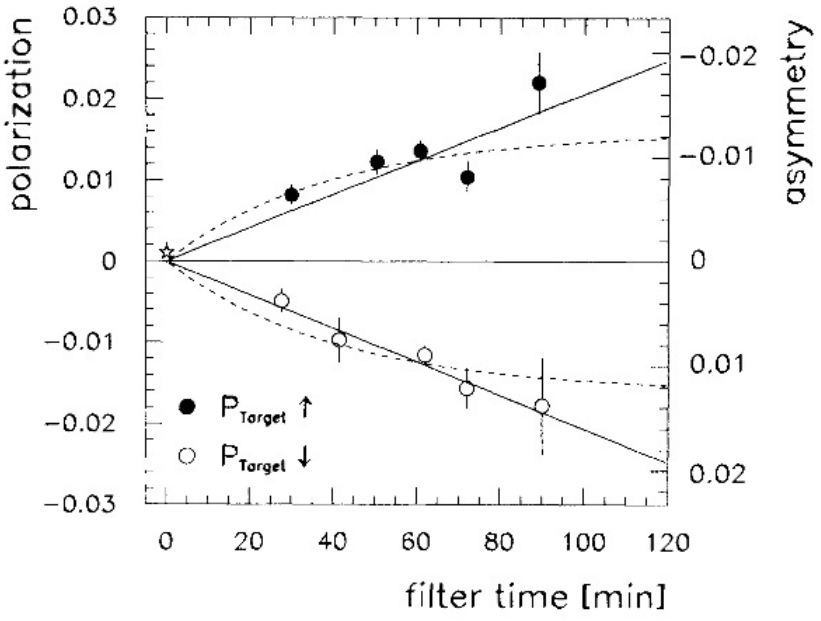

FIGURE 3.5: FILTEX Experiment Results: Asymmetry(right-hand scale) and polarization (left-hand scale) measured after filtering the beam in the TSR for different times.

Low-β quadrupoles have been installed in the target section in order to increase the acceptance angle. The beam lifetime of roughly 30 minutes of an electron cooled beam was achieved. After the filtering time between 30 and 90 minutes, the beam polarization was measured by making use of the large spin correlation coefficient

$A_{xx} = -0.93$ in proton-proton elastic scattering [2]. The pp elastic count rates were measured with scintillation counter telescopes located at $\theta_{lab} = 33^{\circ}$above and below the plane of the storage ring. The result was that the rate of polarization buildup is

$$\frac{\Delta P_b}{\Delta t} = \pm(1.24 \pm 0.06)10^{-2}h^{-1} \tag{3.12}$$

and it implies $\tau_1 = 80$ hours. On Fig. 3.5 the solid lines are based on an assumed rate of polarization build-up of $1.24 \cdot 10^{-2}h{-}1$. The dashed lines are based on the expected build-up rate (τ_1= 42 h) and an assumed polarization lifetime of $\tau_p = 81$ min

Chapter 4

Experimental Setup

4.1 COSY

COSY (Cooler Synchrotron), situated at the Juelich Research center, serves the quests of the fundamental research in the Institute of Nuclear Physics. The acceleration process of the COSY beam consists of several stages.

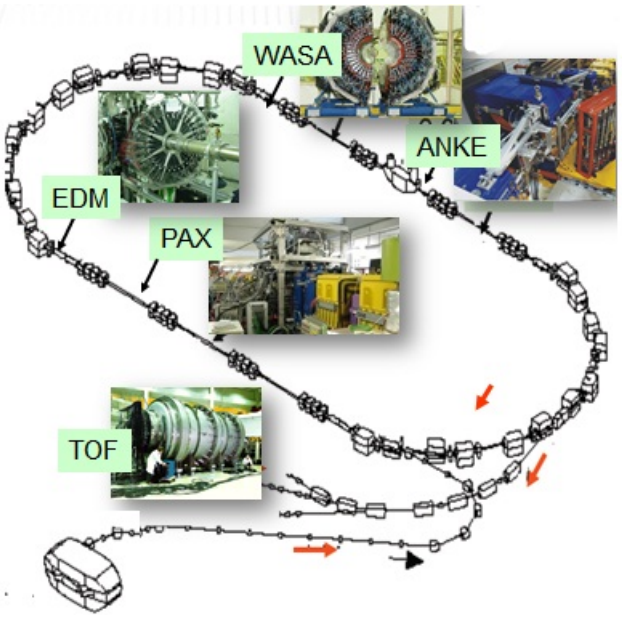

FIGURE 4.1: COSY Ring

Negative ion sources produce unpolarized and polarized hydrogen and deuterium ions, which are then accelerated by JULIC cyclotron up to 300 MeV/c for H^- and

up to 600 MeV/c for D^-, these pre-accelerated ions are stripped off their electrons and the remaining protons or deuterons are injected in COSY ring with 183.4 m circumference, here particles can be accelerated and stored at any momentum in the range from 300 MeV/c to 3.65 GeV/c.

Today unpolarized and transversely polarized beams are available, but in near future beams with longitudinal polarization will also be available after the installation of Syberian Snake. Transversely polarized proton beams are available with intensities up to $1 \cdot 10^{10}$ particles with a typical polarization of 70 %. For deuterons an intensity of $3 \cdot 10^{10}$ with vector and tensor polarization of more than 70 % and 50 % were achieved respectively. The two 40m long straight sections are designed to serve the internal experiments such as WASA(Wide Angular Shower Apparatus), ANKE (Apparatus for studies of Nucleon and Kaon Ejectiles) and PAX target section. The beam can also be extracted for external experiments like TOF (Time Of Flight spectrometer).

4.1.1 Cooling systems

The terms temperature and cooling of a particle beam have been deduced from the kinetic gas theory. The beam temperature is defined by the mean kinetic energy of the particles in the beam in the reference frame, that moves with the mean particle velocity.

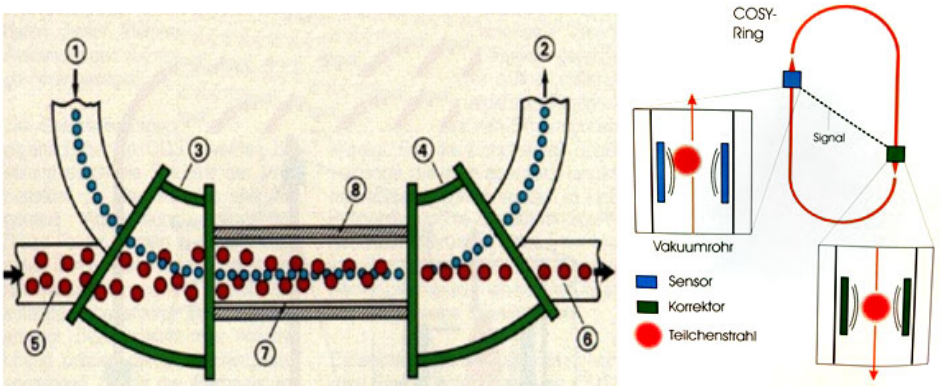

FIGURE 4.2: Schematic drawing of cooling techniques: electron cooling (left), stochastic cooling (right)

Scattering processes cause a beam to change its phase space distribution, for example multiple scattering increases emittance and momentum distribution. Since these effects lead to the losses of beam intensity in time, they should be compensated by so called "cooling" techniques. A 100 keV electron cooler and stochastic cooling above 1.5 GeV/c provide phase space cooling of the stored beam at COSY.

For electron cooling high quality electron beam is injected into the straight section for a certain length. By high quality we mean, that electrons' velocities spread is 1/100 000 of the average velocity, while this average velocity is close to the average velocity of the proton beam; and that electron beam current is much larger than the one of protons. Even though such cooling provides good results (reducing transverse components of the momentum) it is difficult to accelerate an intense beam of electrons for more than 100 kV.

That is why for higher energies stochastic cooling technique is used, which proceeds as follows: Sensor detects the average position of circulating particles with respect to a central orbit and sends signal proportional to the displacement to another point on the ring, where corrective pulse forces the particle to approach the central orbit.

4.1.2 Vacuum System

The polarization build-up in spin-filtering experiments at COSY is known to be small. The long filtering time and the fact that a significant part of the beam is removed on purpose require an ultra-high vacuum in the COSY ring in order to minimize additional losses and to achieve reasonable beam intensities after filtering.
The newly installed NEG pump below the target chamber with the activation of the neighboring NEG (Non Evaporable Getters) coated tubes provided excellent vacuum conditions at COSY. The measured beam-lifetime during the spin-filtering cycles was more than 8000 s, exceeding the expectations.

4.2 PAX section

PAX section represents the interaction point of the beam and polarized target. That is the place where the actual spin-filtering takes place. The experiment set-up requires Polarized Internal gas Target (PIT), consisting of ABS (Atomic Beam Source), the target storage cell, Breit-Rabi Polarimeter (BRP) and Target Gas Analyzer (TGA).

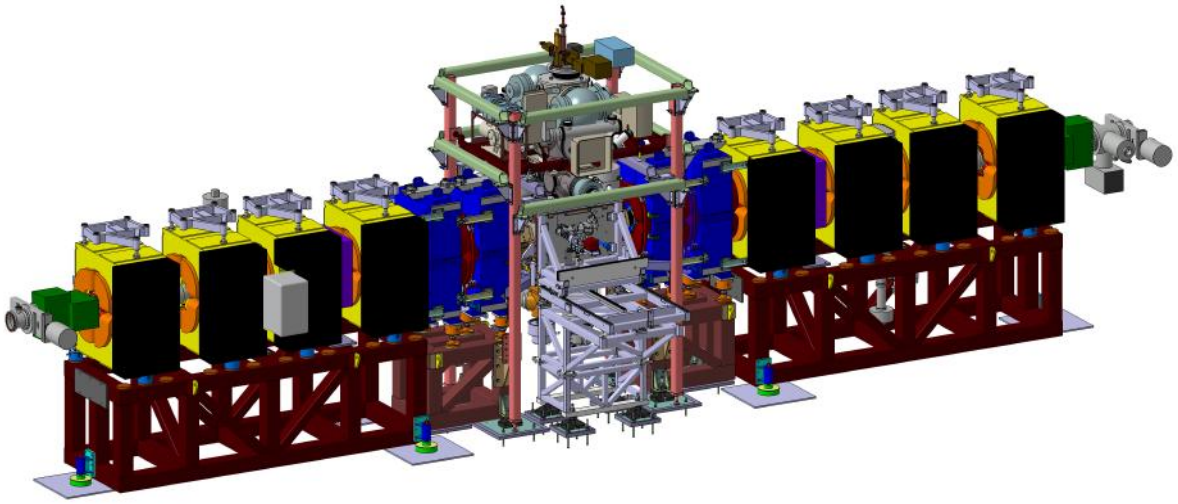

FIGURE 4.3: PAX installation at COSY

4.2.1 Atomic Beam Source

Atomic beam source provides the polarized atoms of hydrogen or deuterium. The dissociator generates atomic hydrogen or deuterium by dissociating molecules in a gas discharge, which is sustained in a microwave induced low ionized plasma. In order to inject fully polarized atoms into the cell the ABS has to perform a selection of the different hyperfine states. For hydrogen, with nucleus having spin 1/2, the quantum numbers for the total angular momenta are F = 1,0. The level F = 1 is a triplet with $m_F = +1, 0, -1$ an the level F = 0 is a singlet with $m_F = 0$.

The $|F, m_F>$ basis is used to describe hyperfine structure.

$$\begin{aligned}
|i> &= |F, m_F> = |m_S, m_I> \\
|1> &= |1, +1> = |+\frac{1}{2}, +\frac{1}{2}> \\
|2> &= |1, 0> = \frac{1}{\sqrt{2}}\left(|+\frac{1}{2}, -\frac{1}{2}> + |-\frac{1}{2}, +\frac{1}{2}>\right) \\
|3> &= |1, -1> = |-\frac{1}{2}, -\frac{1}{2}> \\
|4> &= |0, 0> = \frac{1}{\sqrt{2}}\left(|+\frac{1}{2}, -\frac{1}{2}> - |-\frac{1}{2}, +\frac{1}{2}>\right)
\end{aligned} \tag{4.1}$$

where $m_S = 0$ and $m_I = 0$ are spin projection quantum numbers for proton and electron. In a weak magnetic field as for the PAX experiment, the mixed states

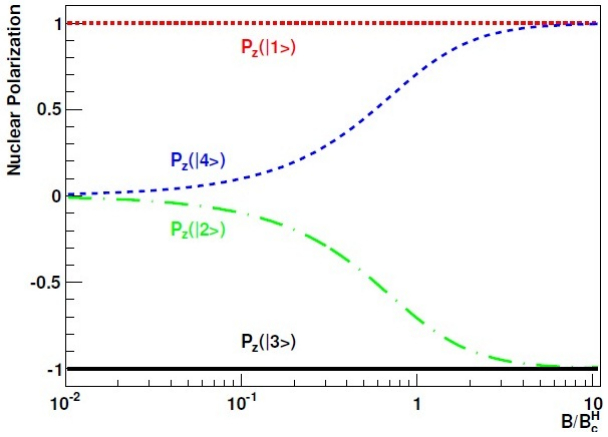

FIGURE 4.4: Nuclear polarization of the hyperfine states of hydrogen versus the external H magnetic field normalized to the critical field $B_c = 50.7$ mT.

$|2>$ and $|4>$ do not contribute to the polarization. Therefore in order to perform the selection of hyperfine states in such a way, that the polarized gas will consist of state $|1>$ only, the ABS consists of a set of sextupole magnets, followed by RF-transition units and two more sextupole magnets. The first set of sextupoles removes states $|3>$ and $|4>$ by deflection, afterward an MFT (Medium Field Transition Unit) exchanges the population numbers between $|2>$ and $|3>$ states. Since the population of state $|2>$ is almost zero, after removal of state $|3>$ by the second set of sextupoles, only hyperfine state $|1>$ remains. [19]

ABS is connected to the storage cell, the purpose of which is to increase the time

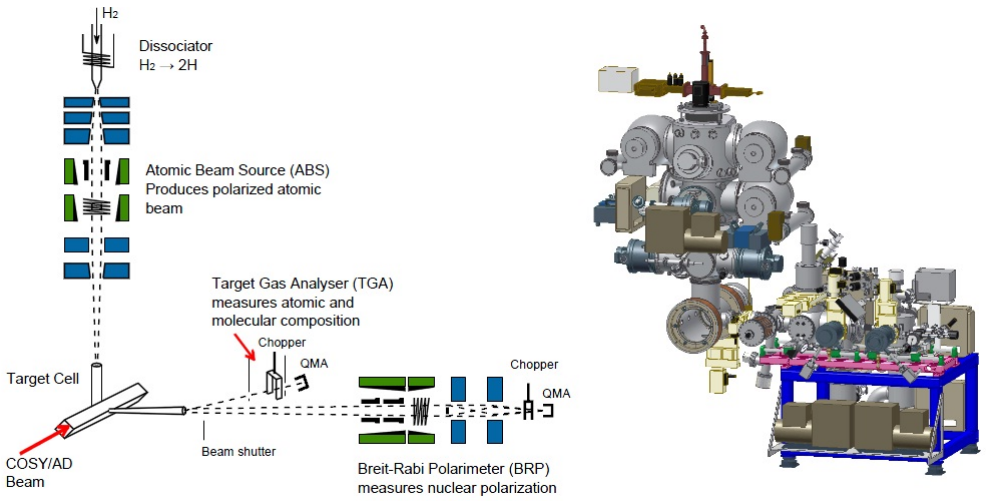

FIGURE 4.5: Schematic drawing of the Polarized Internal Target with the Atomic Beam Source feeding the storage cell, the Breit-Rabi Polarimeter and the Target Gas Analyzer (left). Three dimensional drawing of the ABS and the BRP (right)

of the target gas atoms within the area of the beam, and thus increase the target density. The operation of the polarized target requires a magnetic guide field system providing fields at the storage cell.

4.2.2 Target Gas Analyzer and Breit-Rabi Polarimeter

The Breit-Rabi Polarimeter (BRP) serves to measure and monitor the target polarization. A tube connected horizontally to the storage cell extracts a small fraction of less than 10% of the polarized gas toward the BRP, which measures the relative populations n_i of the hyperfine states, hence is capable to determine the polarization of the target atoms. This serves as important online monitor of the ABS and target storage cell performance. Target Gaz Analyzer measures the relative amount of atoms and molecules coming from the cell. [20]

4.3 ANKE section

ANKE section is responsible for measuring the beam polarization in the spin-filtering experiment. It consists of unpolarized deuteron cluster target and from

Silicon Tracking Telescopes (STTs) which surround the target from two sides.

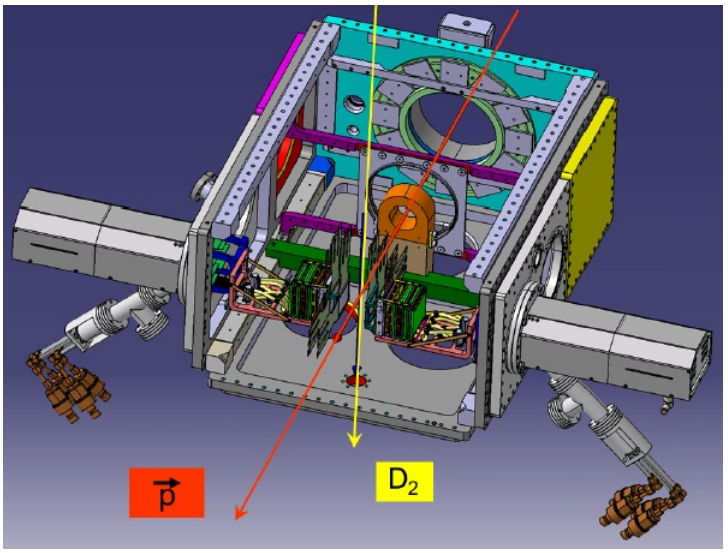

FIGURE 4.6: ANKE set-up: two Silicon Tracking Telescopes installed close to the beam-target overlap region. The polarized proton beam (red) enters the chamber and hits the deuterium cluster target, which is injected from the top (yellow).

4.3.1 Deuterium Cluster Target

Deuterium clusters are produced at the Laval-nozzle as following: adiabatic expansion of the cooled beam (20 K) further cools down the beam and the oversaturated gas spontaneously condensates to clusters. Finally the cluster beam is separated from the residual gas by a skimmer. A deuterium cluster target provides a tar-

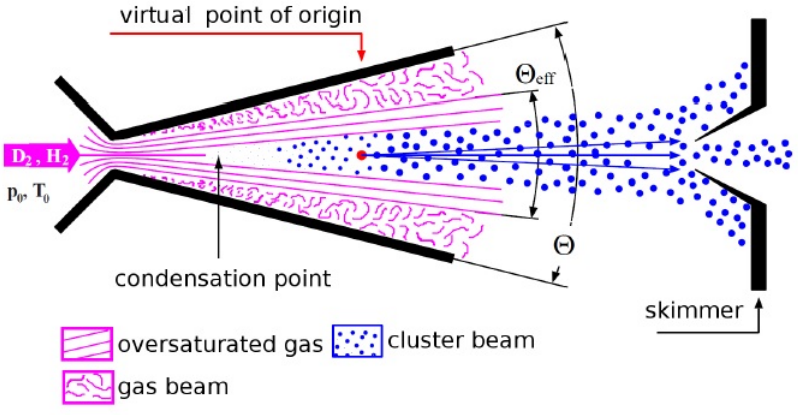

FIGURE 4.7: Cluster production at the Laval-nozzle

get beam of about 10 mm diameter with homogeneous density distribution and a

small beam target overlap region. The absolute density can be varied over a range of about two orders in magnitude ($10^{13} - 10^{15}$ atoms/cm^2), which enables to find compromise between event rates and beam lifetime.

4.3.2 Silicon Tracking Telescopes

The positioning of the detectors has been optimized to measure the beam polarization from proton-deuteron elastic scattering. The setup was build in a ϕ-symmetric (left-right) arrangement to the beam-target overlap to make use of the double ratio method. The determination of the left-right asymmetry in proton-deuteron elastic scattering and the knowledge of the corresponding analyzing power makes it possible to extract the polarization of the proton beam.

Each STT consists of three individual double-sided silicon strip detectors of different thickness. The basic configuration has a 65 μm first layer, a 300 μm second layer and to ensure stopping of protons with kinetic energy up to 40 MeV, a third layer of 5100 μm thickness. The detectors are placed close to the beam target overlap region inside the beam vacuum. A schematic view of the detection system

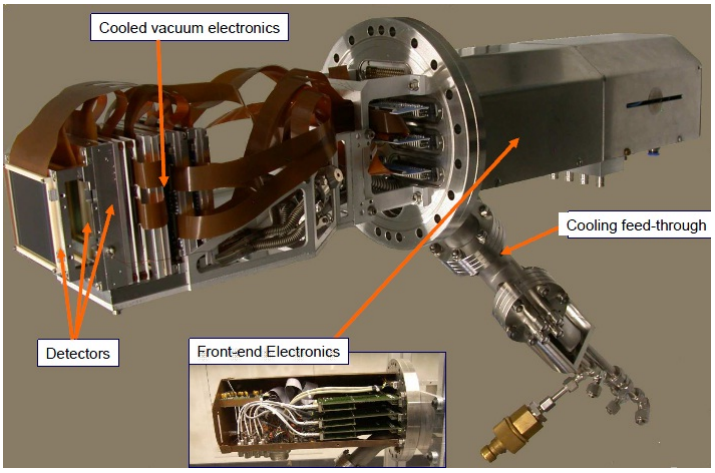

FIGURE 4.8: Silicon Tracking Telescope

build from two STT's is given in the Fig. 4.9 The first layer is placed 28mm from the center of the beam pipe. The distance between the two first layers is set to 20mm. The complete setup is moved 17,5mm downstream.

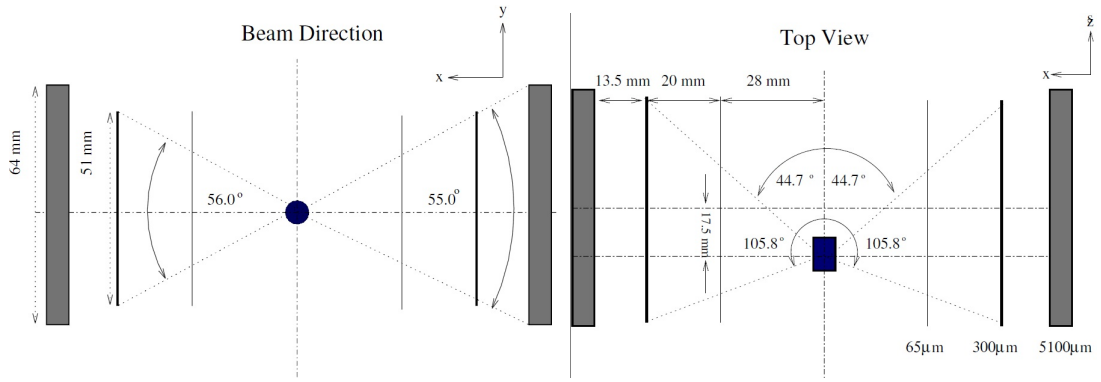

FIGURE 4.9: Geometry of the telescope

This configuration fulfills the requirement of particle identification together with a precise energy determination (1-5%) and tracking with vertex resolution of 1 mm over a wide range. The time resolution of the set-up is less than 1 ns.

Chapter 5

Spin-Filtering Experiment in August-October 2011

The individual components of the experimental apparatus have already been described in the previous chapter. In this chapter we are going to describe the proceedings of the Spin-Filtering experiment at COSY. An overview of the COSY machine with all the installations, needed for the experiment is shown in Fig. 5.1.

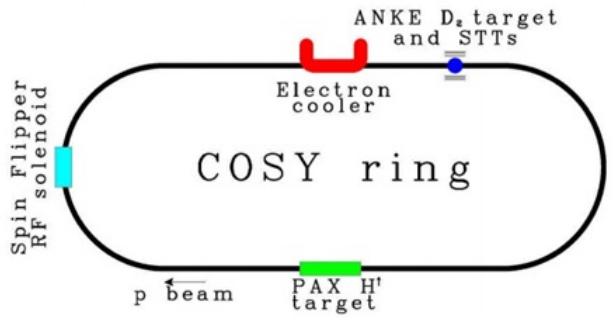

FIGURE 5.1: An overview of COSY machine with all the installations

The polarized hydrogen gas target is installed at the PAX interaction point. The deuterium cluster target, surrounded by the detector system based on Silicon Tracking Telescopes (STTs) is used for the measurement of the beam polarization. Phase space cooling of the stored beam is achieved by Electron Cooler, and the polarization alignment of the stored beam can be reversed using the Spin Flipper

solenoid. During the beam time several types of cycles were performed: spin-filter and zero measurement cycles with unpolarized beam and spin-flipper efficiency and polarization lifetime measurement cycles with polarized beam.

5.1 Spin-Filtering Runs

A typical spin-filtering cycle, consisting of the following steps, is depicted in Fig. 5.2

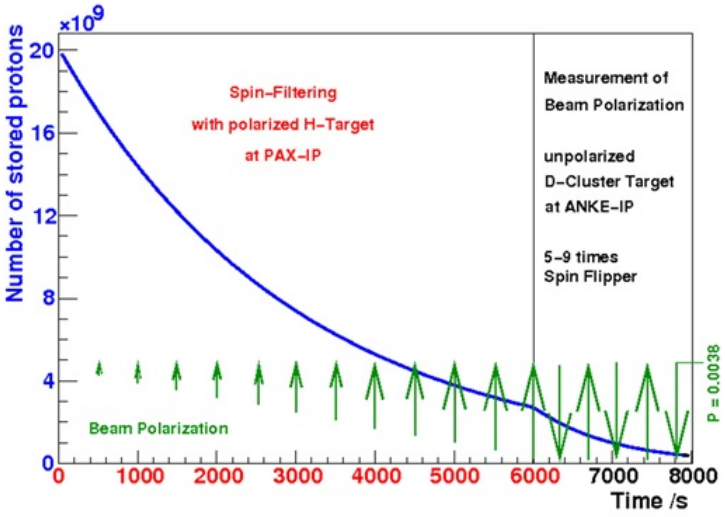

FIGURE 5.2: Typical Spin-Filtering Cycle

◦ An unpolarized proton beam is injected in the COSY ring and is cooled and accelerated to 49.3 MeV. This energy has been chosen for the spin-filtering experiments, because of existing of the analyzing power in proton-deuteron elastic scattering The typical number of particles injected and accelerated in every cycle was about $5 \cdot 10^9$.

◦ At this point the spin-filtering cycle starts. Polarized hydrogen is injected into the storage cell at the PAX interaction point. The holding field coils are powered on in either up (↑) or down (↓) orientation for the duration of the spin-filtering period. Two different durations for the spin-filtering periods have been adopted: one lasting for 12000 s, and a longer one of 16000 s, corresponding about 1.5 and 2 times the beam-lifetime(8000 s).

∘ At the end of the spin-filtering period, the PAX polarized target is switched off, the ANKE deuterium-cluster target is switched on and the data acquisition of the beam polarization starts. During the beam polarization measurement, the beam polarization is reversed three times using the spin-flipper. This allows for the determination of the induced beam polarization within each cycle thereby reducing systematic errors. ∘ Spin-filtering cycles have been repeated for different directions of the target holding fields: up (↑) or down (↓)

5.1.1 Zero Measurement

In order to provide a zero polarization calibration of the detector, a series of cycles without spin-filtering have been carried out in addition. To be as close as possible to the experimental conditions of a standard spin-filtering cycle, the zero-measurement cycle reflected exactly the same sequence of operations, differing only in the number of injected particles and the duration of the spin-filtering part.

5.1.2 Spin-Flipper Efficiency

Before the measurement, the spin-flipper, which employs a resonant RF-solenoid, has been tuned to the proper working conditions and its efficiency has been measured in dedicated runs. A polarized proton beam was injected in the ring and its polarization was measured, subsequently, the spin-flipper switched on and a total number of 99 spin-flips have been induced on the beam. From the remaining polarization the spin-flipper efficiency has been determined as $\varepsilon_{SF} = 0.987 \pm 0.001$

5.2 Polarization Lifetime Runs

A strong-focusing synchrotron like COSY has two different types of depolarizing resonances: 1) imperfection resonances, caused by magnetic field errors and misalignments of the magnets and 2) intrinsic resonances excited by horizontal

fields due to the vertical focusing. Intrinsic resonances arise when there is simple relation between the spin tune and the vertical betatron tune. Depolarizing resonances may also arise due to a simple relation between spin tune and orbit or the synchrotron frequency. Here, spin tune is the net precession angle of the particle's magnetic moment during one turn in the machine. To quantify these effects, a dedicated measurement of the polarization lifetime with polarized beam was performed. A cycle starts with injection of a polarized proton beam from the polarized source of COSY.

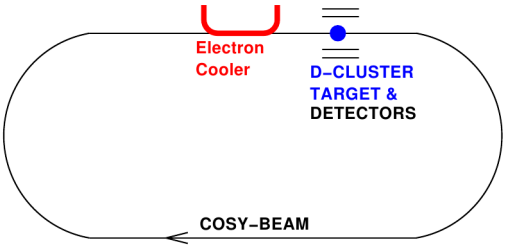

FIGURE 5.3: An overview of COSY machine with all the installations, needed for polarization lifetime measurement

Then the beam is cooled via electron cooling and accelerated to 49.3 MeV. data is taken, using beam scattering on deuterium target at ANKE section. After measuring for about 300 s the cluster target is switched off for about 5000 s in order to decrease the beam loss during the waiting period, and finally is switched on again for approximately 1000s. The time periods are optimized to yield the smallest relative errors in τ_{Pol}, statistical error of both measurements are equal. These are the polarization lifetime runs, that are used for the analysis described in the next chapter. The main task was to measure polarizations at the begining and at the end of the cycles, using double ratio method on pd elastic scattering.

The measured beam polarizations before and after waiting allow one to determine the polarization lifetime and conclude about its influence on polarization build-up. For this purpose deuteron break-up reaction is a by-product, but since rather a big amount of data was gathered, break-up events were also separated and analyzed for investigating reaction analyzing power and contributing to experimental data, that can be used as input for the Chiral Perturbation Theory.

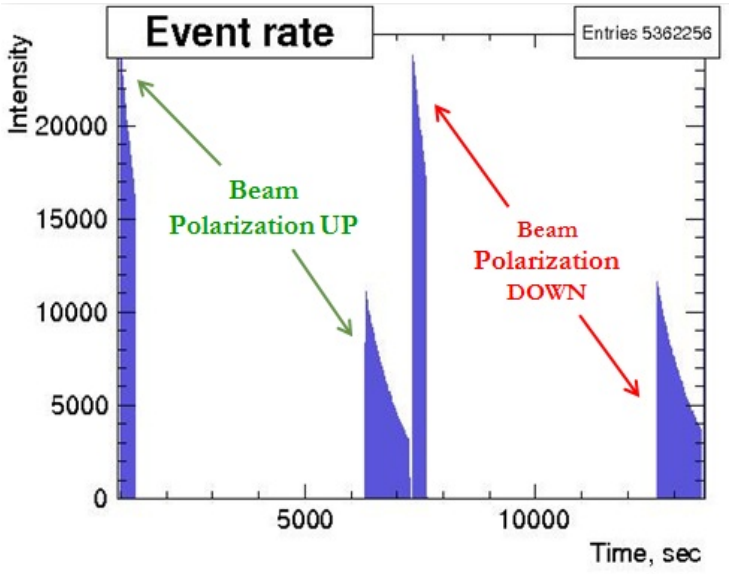

FIGURE 5.4: Event rate in two consequitive cycles of polarization lifetime measurements

Chapter 6

Data Analysis

In order to describe the procedure of data analysis, we start with presenting coordinate system and doube ratio method, according to Gerald and Ohlsen paper. And continue with description of procedures, undertaken on various steps of analysis, including particle identification, reaction separation and measurement of polarization. Result of polarization lifetime calculation is presented and discussed. In addition, investigation of deuteron breakup analyzing power is scrutinized.

6.1 Coordinate System and Polarization Specifications

In the data analysis Cartesian coordinate system is formed with z along the incident beam momentum $\mathbf{k_{in}}$, y along $\mathbf{k_{in}} \times \mathbf{k_{out}}$ where $\mathbf{k_{out}}$ is scattered particle momentum, and x such as to define a right-handed coordinate system. Let's define $\mathbf{l}, \mathbf{n}$ and $\mathbf{k}$ unit vectors pointing along the x, y and z coordinate axes respectively. So, $\mathbf{k} = \mathbf{k_{in}}/k_{in}$, $\mathbf{n}||(\mathbf{k_{in}} \times \mathbf{k_{out}})$, and $\mathbf{l}||(\mathbf{k} \times \mathbf{n})$. The unit vector pointing along the spin quantization axis is denoted by $\mathbf{s}$; its direction is defined in terms of β, the angle between $\mathbf{s}$ and beam direction, and ϕ, the angle between its projection on xy plane and y axis.

In this system, the scattering is always in the xz plane, and the momentum vector

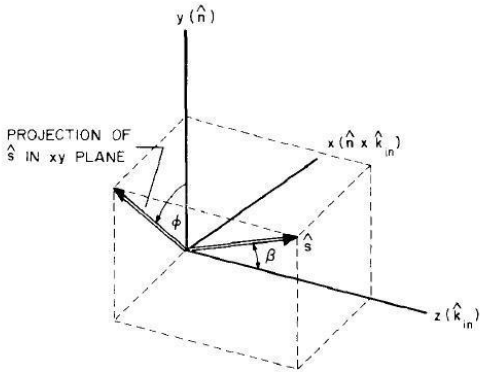

FIGURE 6.1: Definition of the Spin Angles

of the scattered particle lies in the xz half-plane with positive x. The direction, called "up" is defined by the transverse component of spin quantization axis. $\mathbf{s}_\perp = \mathbf{s} - (\mathbf{s}\cdot\mathbf{k})\mathbf{k}$. Hence according to an observer who is looking along the beam direction and is aligned with "up" direction, the scattering (positive x half-plane of xz plane) is to the left, if y axis is along $\mathbf{s}_\perp$ ($\phi = 0°$). Correspondingly if $\phi = 180°$, $\phi = 270°$and $\phi = 90°$, then the scattering is to the right, up and down, respectively. [21]

6.2 Double Ratio Method

The cross section for a polarized beam of spin 1/2 particles is

$$\sigma(\theta,\phi) = \sigma_0(\theta)[1 + p_y A_y(\theta)] \tag{6.1}$$

where $\sigma_0(\theta)$ is the cross section for the scattering of an unpolarized beam at the scattering angle θ, $A_y(\theta)$ is "the analyzing power" of the *reaction* at the same angle and p_y is the y component of the beam polarization:

$$p_y = \mathbf{p}\cdot\mathbf{n} \equiv \mathbf{p}\mathbf{sin}\beta\mathbf{cos}\phi \equiv \mathbf{p}_\perp\mathbf{cos}\phi \tag{6.2}$$

where $\mathbf{p}$ is the beam polarization, $\mathbf{n}$ is unit vector along the y axis, and $p_\perp$ is the component of beam polarization perpendicular to its direction of motion. Since in our experiment we have transversely polarized beam, we assume $\beta \approx 90°$. Hence

the difference between $p_\perp$ and p is neglected, and we set $p_\perp \equiv p$.

The actual number of counts recorded in a detector is

$$N(\theta, \phi) = nN_t\Omega E\sigma(\theta, \phi) \tag{6.3}$$

where n is the number of particles, incident on the target, N_t is the number of target nuclei per cubic centimeter, Ω is a geometrical factor, defined by the detector, i.e. the solid angle subtended by the detector, and E is the detector efficiency. It is allowed, that solid angle factor as well as its efficiency of detector 1 to be different from those of detector 2. Therefore Eq. 6.3 for each detector will look like

$$N_1(\theta, \phi) = nN_t\Omega_1 E_1\sigma_0(\theta)[1 + p_y A_y(\theta)cos\phi] \tag{6.4}$$

$$N_2(\theta, \phi) = nN_t\Omega_1 E_2\sigma_0(\theta)[1 + p_y A_y(\theta)cos\phi] \tag{6.5}$$

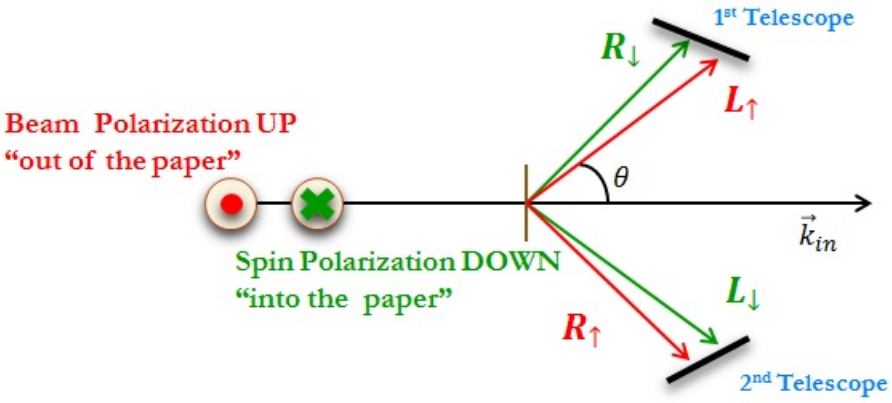

FIGURE 6.2: Two-detector idealistic symmetric arrangement

On Fig. 6.2 spin direction "up" is depicted coming out of paper in red, hence detector 1 detects particles, that are scattered to the "left" ($\phi = 0°$) and detector 2 gets particles that are scattered to the "right" ($\phi = 180°$). Therefore,

$$N_1(\theta, 0) \equiv L_1 = nN_t\Omega_1 E_1\sigma_0(\theta)[1 + p_y A_y(\theta)] \tag{6.6}$$

$$N_2(\theta, \pi) \equiv R_2 = nN_t\Omega_1 E_2\sigma_0(\theta)[1 - p_y A_y(\theta)] \tag{6.7}$$

If we now "flip" the polarization $\mathbf{p} \to -\mathbf{p}$, spin "up" direction will be going into the paper(depicted in green), detector 1 will be on the right and detector 2 on the left side.

$$N_1(\theta, \pi) \equiv R_1 = n' N_t' \Omega_1 E_1 \sigma_0(\theta)[1 - p_y A_y(\theta)] \tag{6.8}$$

$$N_2(\theta, 0) \equiv L_2 = n' N_t' \Omega_1 E_2 \sigma_0(\theta)[1 + p_y A_y(\theta)] \tag{6.9}$$

Primes are used to indicate that the integrated charge and the effective target thickness may not be the same for the two runs. In te following analysis description the latter case is referred to as beam polarization "down". We can form geometrical means of number of particles scattered to the left $L \equiv \sqrt{L_1 L_2}$ and particles scattered to the right $R \equiv \sqrt{R_1 R_2}$.

$$L = [nn' NN' \Omega_1 \Omega_2 E_1 E_2]^{\frac{1}{2}} \sigma_0 [1 + pA_y(\theta)] \tag{6.10}$$

$$R = [nn' NN' \Omega_1 \Omega_2 E_1 E_2]^{\frac{1}{2}} \sigma_0 [1 - pA_y(\theta)] \tag{6.11}$$

We can solve for $pA_y(\theta)$ and get left-right assymetry ε

$$\varepsilon = \frac{L - R}{L + R} = \frac{2pA_y [nn' NN' \Omega_1 \Omega_2 E_1 E_2]^{\frac{1}{2}} \sigma_0}{2[nn' NN' \Omega_1 \Omega_2 E_1 E_2]^{\frac{1}{2}} \sigma_0} = pA_y(\theta) \tag{6.12}$$

which is independent of relative detector efficiencies (E_1, E_2), solid angles (Ω_1, Ω_2), relative integrated charge (nn') and target thickness variations. (NN'). n and N, quantities common to the two channels, are averaged over the data acquisition time (in one run) E and Ω, quantities different in two channels, must not vary with time. We can define the geometric mean of the number of particles detected by detector 1 in two runs as N_1

$$N_1 \equiv \sqrt{L_1 R_1} = \Omega_1 E_1 \sigma_0(\theta) NN' nn' [1 - (pA_y)^2]^{\frac{1}{2}} \tag{6.13}$$

and for particles detected by detector 2 we have

$$N_2 \equiv \sqrt{L_2 R_2} = \Omega_2 E_2 \sigma_0(\theta) NN' nn' [1 - (pA_y)^2]^{\frac{1}{2}} \tag{6.14}$$

Monitoring on the ratio

$$\frac{N_1}{N_2} = \frac{\Omega_1 E_1}{\Omega_2 E_2} \tag{6.15}$$

provides the check on the performance of the apparatus; this variable is required to be constant in time if the asymmetry determination is to be accurate. Dead time of the counting devices may be either common or different for the two chanels or not, depending on the equipment used. In our experiment, all the detectors are connected to one Data Acquisition System, so dead time is the same for all detectors. Generally, if it is not common, a correction factor must be used. The statistical error associated with a measurement of the assymetry ε is given by means of geometrical means L and R. (See Appendix A).

$$\delta\varepsilon = \sqrt{\frac{1-\varepsilon^2}{L+R}} \tag{6.16}$$

6.3 Track Reconstruciton

Tracks were reconstructed starting from the hits in the second layer. Combinations of these hits with the hits in the first layer have been considered. If the reconstructed track hits the inside the ellipse of beam-target overlay in ZOY plane (at $x = 0$), then it is stored. In general, the hit from 3-rd layer is also added to the reconstructed track in case it is inside the 20°cone along the track with the apex at the 2nd layer hit. The cone opening angle corresponds to the maximum angle of multiple scattering. The 3rd layer hit doesn't change a track geometry, it is used only to fulfill the energy deposit information. Root files with reconstructed tracks was provided by Gogi Macharashvili [22].

6.4 Elastic Scattering Identification

Experiments were held with proton beam with kinetic energy of 49.3 MeV hitting the deuterium cluster target. This energy is under the threshold of π production. That's why at this case only two channels of reaction are possible, pd $\rightarrow$ pd elastic

scattering and pd → ppn deuteron breakup.

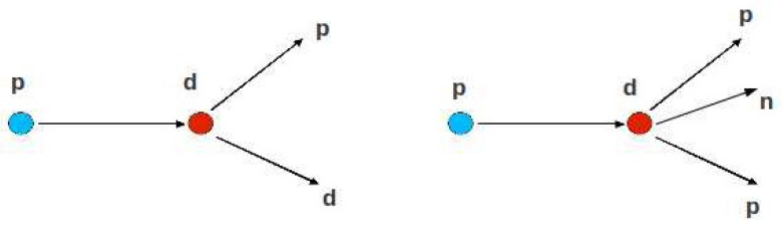

FIGURE 6.3: Possible chanels of proton deuteron reactions

In order to determine elastic events several steps were undertaken:

6.4.1 Investigating energy deposits dependences.

The energy deposit in different layers of silicon detector is dependent on the energy of the scattered particle and its type, according to Bethe's Formula.

$$-\frac{dE}{dx} = \frac{4\pi}{m_e c^2}\frac{nz^2}{\beta^2}\left(\frac{e^2}{4\pi\varepsilon_0}\right)^2\left[ln\left(\frac{2m_e c^2\beta^2}{I(1-\beta^2)}\right)-\beta^2\right] \tag{6.17}$$

where $\beta = v/c$, v is velocity, E is energy of the particle; x is the distance traveled by the particle; c is speed of light; and $z\,e$ is particle charge; where e is the charge of the electron; m_e is mass of the electron; n is electron density of the target; I is the mean ionizaiton energy of the target; while ε_0 is the vacuum permittivity.
The basic ideas of the above mentioned formula are that 1)the bigger charge the particle has, the more rapid is the energy loss and 2) the faster particle is, the less energy it loses per distance unit. Hence from the energy deposits in the detector layers it is possible to distinguish deuterons behavior from the one of protons, and to make conclusion whether this particle was stopped or not, i.e. is it lost all its initial kinetic energy, while passing through the matter.

On Fig. 6.4 (upper, left) there are shown the energy deposit two-dimensional distributions for particles, that were detected only in first two layers of the detector, In order to ease the graphical cut appliance, the new parameter was introduced. It

allows to transform concentrations in the distribution into horizontal bands. See Fig. 6.4 (lower, left). This is so called **P**article **ID**entification parameter, defined as $PID = (dE_1 + dE_2)^{1.62} - dE_2^{1.62}$.

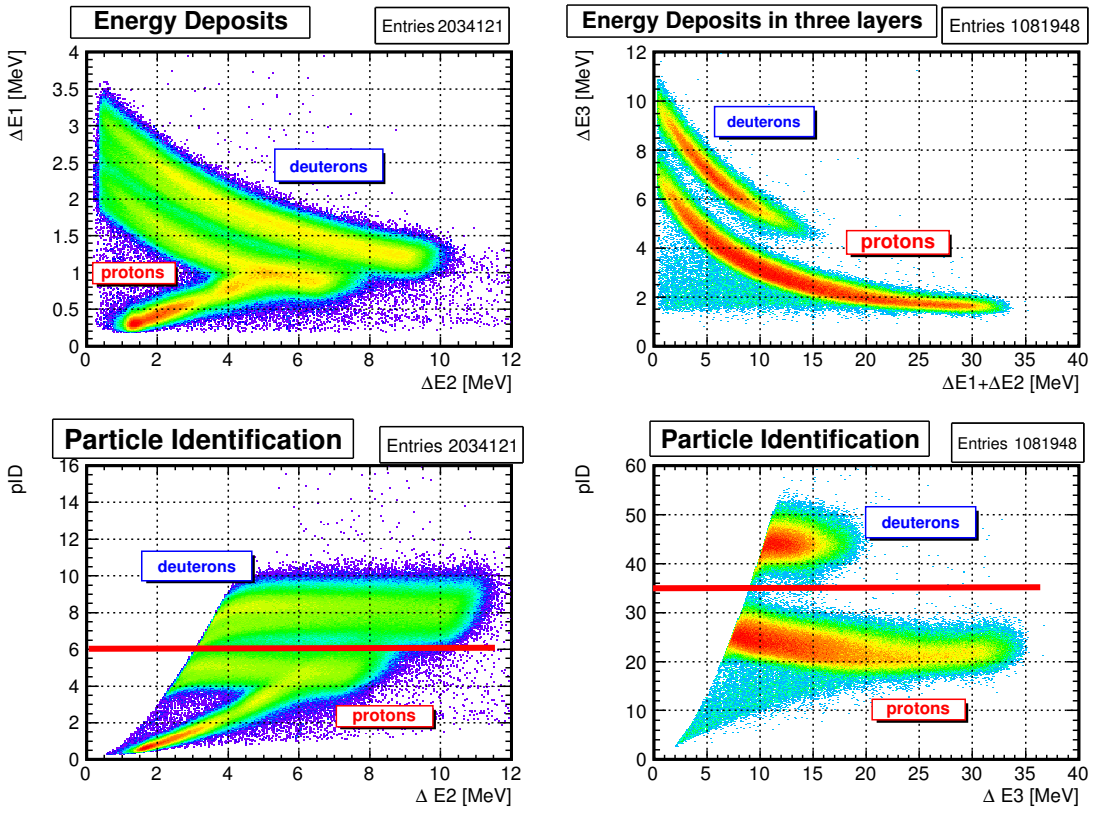

FIGURE 6.4: Energy Deposit in second layer vs the one in the first layer (upper, left) Energy Deposit in Third Layer vs Sum of Energy Deposits in First and Second Layer (upper, right); Corresponding Particle IDentification Index Distributions (lower row)

The upper band corresponds to the stopped deuterons, while the lower horizontal band corresponds to the stopped protons. The part of the distribution with the slope corresponds to particles that were not stopped in the second layer, and didn't hit the third layer of the silicon detector. The latter data points cannot be used, since there is no information about the total kinetic energy.

Similar distributions were produced for particles, that were detected in all three detectors. Sum of energies, deposited in the first and second layers vs. energy deposited in the third layer is shown on Fig. 6.4 (upper, right). In order to apply

horizontal cuts modified definition of PID3 was used

$$PID3 = (dE_1 + dE_2 + dE_3)^{1.62} - dE_3^{1.62} \tag{6.18}$$

These experimental distributions are consistent with those, obtained from GEANT4 simulations, where the information about particle type, its kinematic energy, as well as the properties of the detector are included.
This allows to use following cuts for the identification of stopped deuterons coming from pd elastic scattering: for particles, stopped in 2nd layer PID>7.5, and for those stopped in third layer PID3>37.

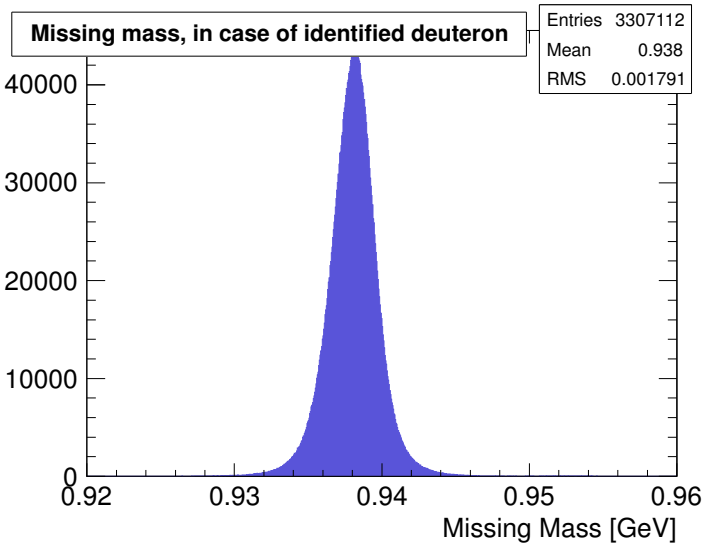

FIGURE 6.5: Missing Mass in case, when stopped deuterons were identified

6.4.2 Reconstructing elastic deuterons from identified protons.

In case the elastic proton is stopped in one of the STTs it is also possible to reconstruct corresponding deuterons' kinematic parameters using the 4-momentum conservation. It's worth noticing, that protons, coming from elastic scattering, stop only in the third layer. So, after eliminating deutron events, the rest of particles detected in the third layer (17<PID3<24) were compared with theoretically

expected kinetic energy, that was deduced from the experimentally given polar angle, assuming the track belongs to proton. That gives the following distribution with distinguished signal near zero (Fig. 6.6 (right)). These stopped particles are considered to be the protons, emitted from pd → pd elastic scattering.

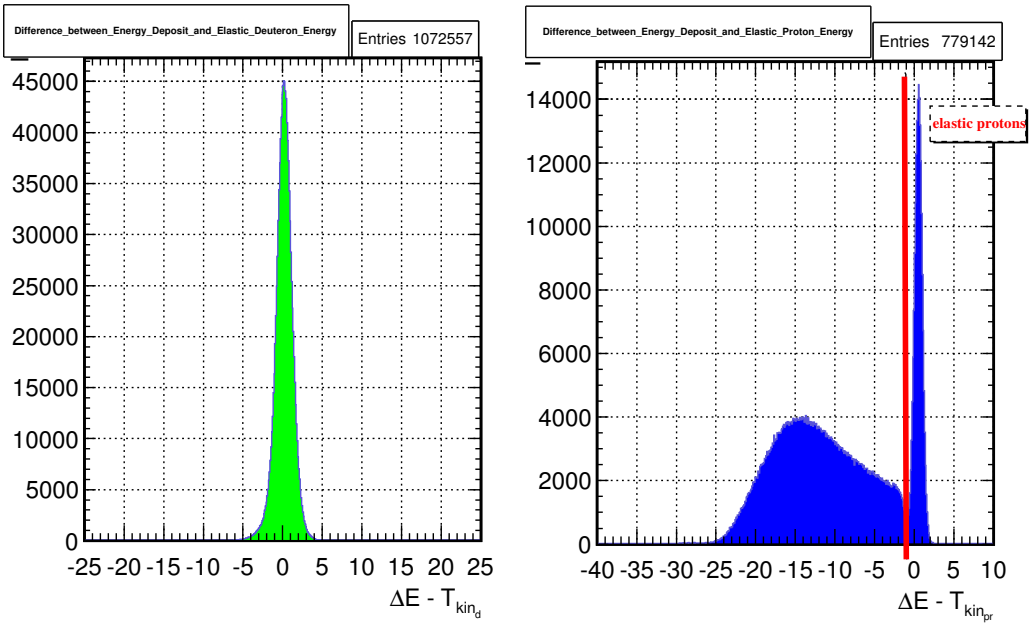

FIGURE 6.6: Differences between Kinetic Energies from Experiment and Theoretical Expectations for stopped identified deuterons (left) for stopped elastic protons after elimination of deuterons (right)

The left part of the distribution corresponds to protons, coming from break-up events, which will be discussed in more detail later.

4-momentum of the detected particle is constructed by assuming the mass of proton, and experimentally measured components of the momentum. Since pd elastic scattering is two-body kinematic problem, it is convenient to use the center of mass coordinate system, where the deuteron and proton momentums are equal and have opposite sign. After assigning the deuteron mass to the reconstructed particle, it is converted back to the laboratory reference frame and recoil deuteron track is added to the count rate of the opposite telescope. The angular range of these 704305 reconstructed deuterons is from 26°to 52°. Even though the number of reconstructed deuterons is 10 times less than the one of detected deuterons, they

have significant weight due to the large values of analysing power in this angular range(see Fig. 6.8).

6.4.3 Control checks for selected particles.

For the cross check, protons and deutrons from elastic scattering, identified according to above mentioned procedures, are compared to the simulation kinetic energy vs. polar angle. The result is shown on the Fig. 6.7 (left), where we see rather good distribution of experimentally identified particles around the expected curves.

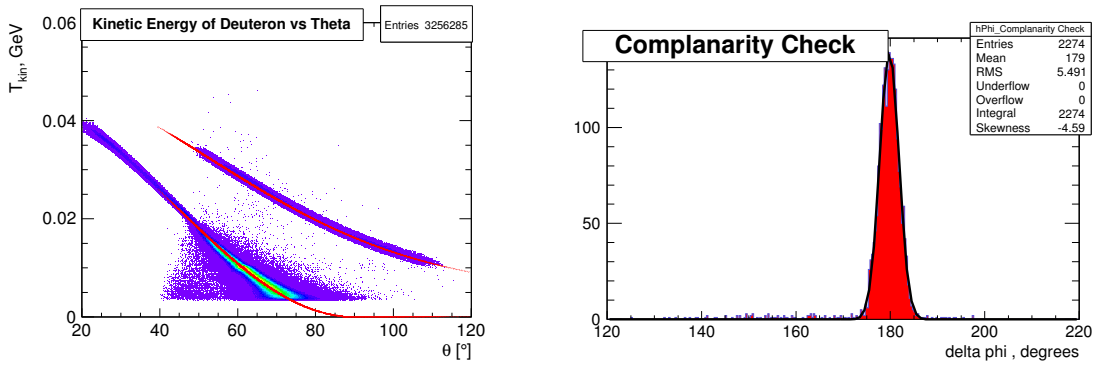

FIGURE 6.7: Kinetic Energy vs Polar Angles (left) Complanarity Check for events, when both elastic deuteron and proton are detected (right)

The geometrical acceptance of current detector set-up (40-120°) provides the region, where proton and deuteron can be detected in the coincidence. These tracks were checked for complanarity. In the Fig. 6.7 (right) distribution of the difference of azimuthal angles of two detected tracks shows peak around 180°with RMS less than 5.5°. This picture confirms that elastic scattering is in one plane as expected.

6.5 Polarization

The energy of the experiment was chosen since analyzing power for pd → pd elastics scattering is well known. The data was taken from King's Article (Fig. 6.8, Appendix C [23]) and was fitted by 5th order polynom. In good approximation,

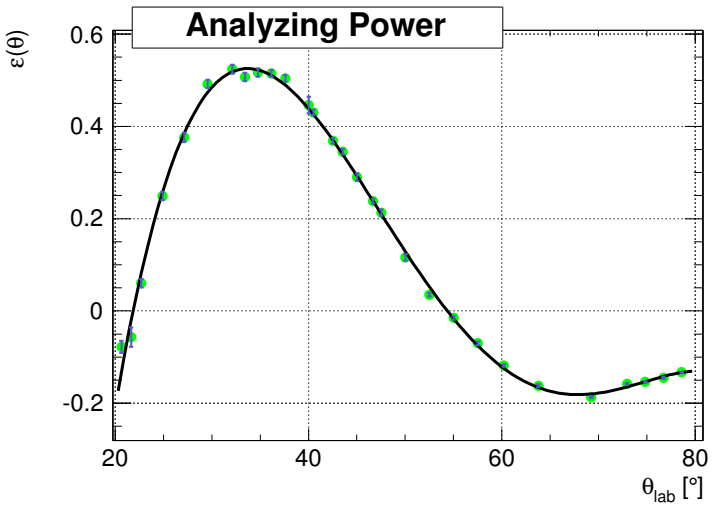

FIGURE 6.8: Interpolated A_y angular dependence used for the beam polarization estimate

analyzing power is constant in each 1°bin. In order to calculate polarization both analyzing power and asymmetry should be known for every given θ interval.
The following formula was used to calculate the beam polarization in each θ_{lab} interval:

$$\varepsilon(\theta) = PA_y(\theta)\langle cos\phi\rangle, \tag{6.19}$$

where ε is count rate assymetry, $A_y(\theta)$ is interpolated angular dependence of the analysing power and ϕ is the azimutal angle of the tracks. For more precise

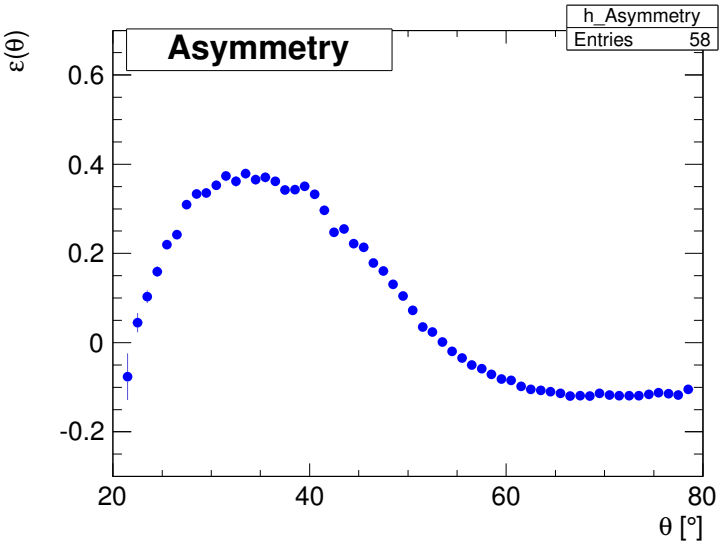

FIGURE 6.9: The asymmetry vs θ_{Lab} for the detected and reconstructed deuteron

results, the average value of theta was obtained for each θ_{Lab} bin and corresponding analyzing power value was used. Average cosϕ was also calculated for each bin to be used in the polarization formula. In Fig. 6.9 the typical asymmetry vs θ_{Lab} for the detected and reconstructed deuterons is presented.

Polarization in 6.19 is the free parameter to fit the assymetry, and gives the same result as polarization calculation bin-by-bin, i.e. by dividing assymetry on analyzing power and averaged cosine.
Considering the structure of analyzed runs, polarization was calculated for the beginning and for the end of cycles separately. After storing period of 5000 s the

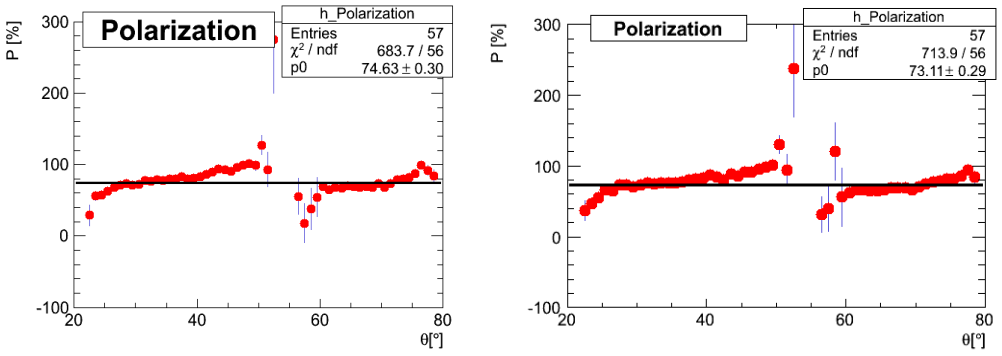

FIGURE 6.10: Polarization for 20504-20509 runs at the beginning and at end of the cycle

polarization loss is about 2,5% for the beam with 74.6% initial polarization.

$$P(t = 5000) = P(0)e^{-\frac{5000}{\tau_{pol}}} \tag{6.20}$$

Solving the equation for beam polarization lifetime gives $\tau_{pol} = 2.5 \cdot 10^5$s.

This means, that for experiments at COSY, where durations of spin filtering runs were 12000 and 16000 s, polarization losses due to depolarization effects can be neglected.

6.6 Identifying break-up events

As was mentioned before there are only two possible channels of reaction, that are detected during the experiment: elastic scattering and pd breakup. After finalizing the analysis of elastic events, identification of pd breakup events was performed.

Since Silicon Tracking Telescopes detect only charged particles, one can only isolate breakup reaction by detecting two protons. Particles with 20<PID3<30 and 4.3<PID<5.7 were used for separating the stopped protons. Breakup, being a three body final state reaction, has larger phase space than the elastic process and there is overlap between these two. Therefore it is important to exclude protons, coming from the elastic scattering.

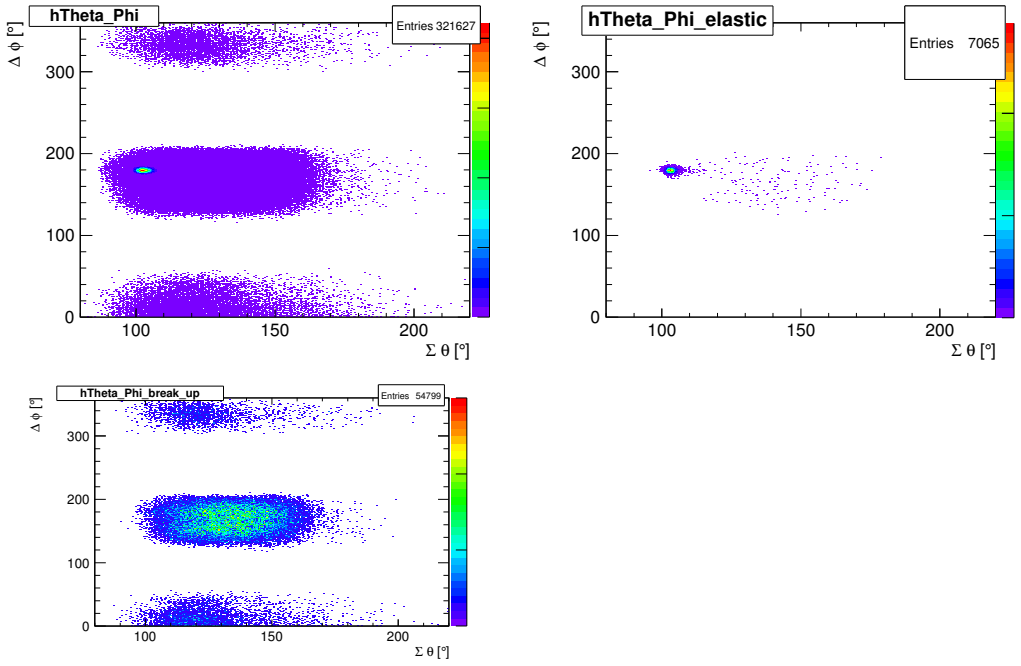

FIGURE 6.11: Polar and Azimuthal Angles Dependences for all two track events (left), when both proton and deuteron come from elastic scattering(right), for identified break-up events (lower)

There are two possible schemes of detected break-up events a) when two protons are scattered at large angles and detected by opposite telescopes and b)when two protons are emitted in the same direction at low relative momentum. It is possible to scrutinize two protons as the the quasi system with all its kinematic variables.

Total momentum of detected proton pair is $\mathbf{P}_{pp} = \mathbf{P}_1 + \mathbf{P}_2$, where $\mathbf{P}_1$ and $\mathbf{P}_2$ denote the proton momenta in center of mass system. The kinetic energy in the rest frame of the proton pair is called excitation energy and is given by

$$E_{pp} = 2(m_p^2 + \mathbf{k^2})^{1/2} - 2m_p \tag{6.21}$$

where **k** and -**k** are the momenta of protons in the rest frame of the proton pair. Break-up reaction can be described by five independent variables, chosen from

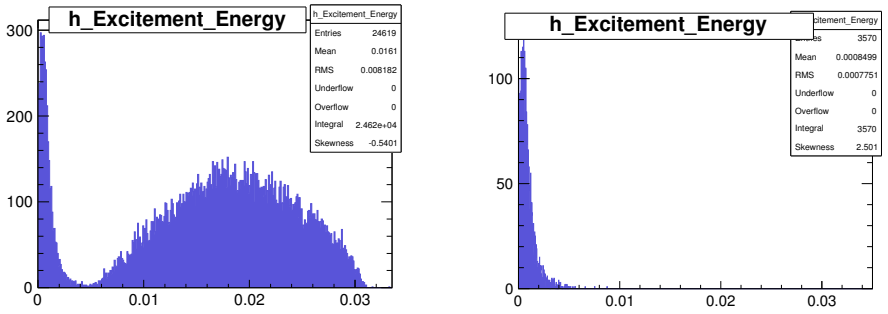

FIGURE 6.12: Excitation Energy Distribution for protons, both detected in STT (left), and particularly when both protons are detected in the same telescope (right)

$\mathbf{p}$, $\mathbf{p_n}$, $\theta_\mathbf{p}$, $\phi_\mathbf{p}$, $\theta_\mathbf{n}$,$\phi_\mathbf{n}$, $\delta\phi_{pq}$, and excitation energy E_{pp}, where n index indicates parameters of reconstructed neutron in center of mass system, while p indicates paremeters of Jakobi momenta, defined as $p = \frac{\mathbf{P_1^{cm}} - \mathbf{P_2^{cm}}}{2}$. As the control criterion we filled the missing mass histogram is produced, which peakes at neutron mass.

Considering all the experimental data, we can reconstruct neutron from 4-momentum conservation

$$n^\mu = p_b^\mu + d^\mu - p_1^\mu - p_2^\mu \tag{6.22}$$

where p_b^μ is the four-momentum of the incident proton, d^μ is the one of deuteron target, and p_1^μ and p_2^μ are the scattered protons, that are stopped in the detectors.

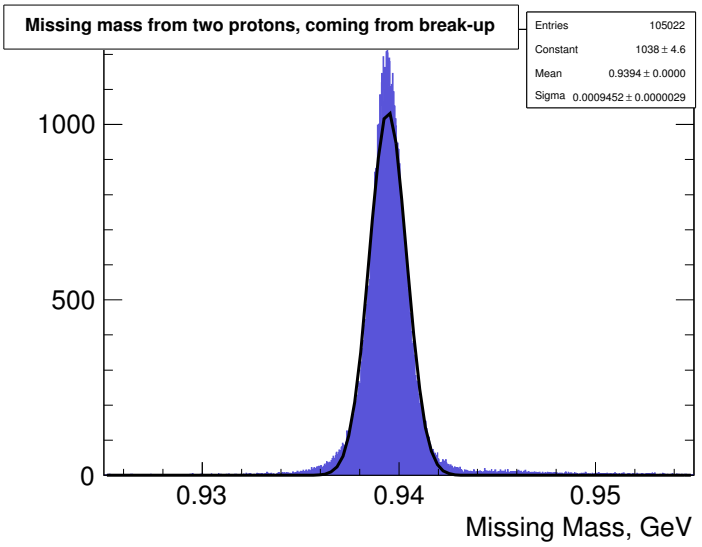

FIGURE 6.13: Missing mass from two break-up protons, stopped in Silicon Tracking Telescopes

6.7 Breakup Analyzing Power

The analyzing power A_y of the reaction can be determined with respect to one of these variables and integrating over the others. For the current case, the measurement of the analyzing power is carried out as function of neutron azimuthal angle. Therefore neutron up/down asymmetry in respect to its azimuthal angle was used to deduce analyzing power [24],

$$A_y(\phi) = \frac{\varepsilon_n(\phi)}{P < cos\phi >} \tag{6.23}$$

ε was calculated as

$$\varepsilon_n(\phi) = \frac{U(\phi) - D(\phi)}{U(\phi) + D(\phi)} \tag{6.24}$$

where U refers to the number of reconstructed neutrons when the beam polarization is "up", and D is the number of reconstructed neutrons when the beam polarization is "down". From this asymmetry, using polarization calculated from elastic scattering, it is possible to calculate analyzing power dependence on azimuthal angle for the break-up reaction.

It is seen, that analyzing power has dependence on azimuthal angle different than just pure cosine. The interpretation of this result is still under discussion.

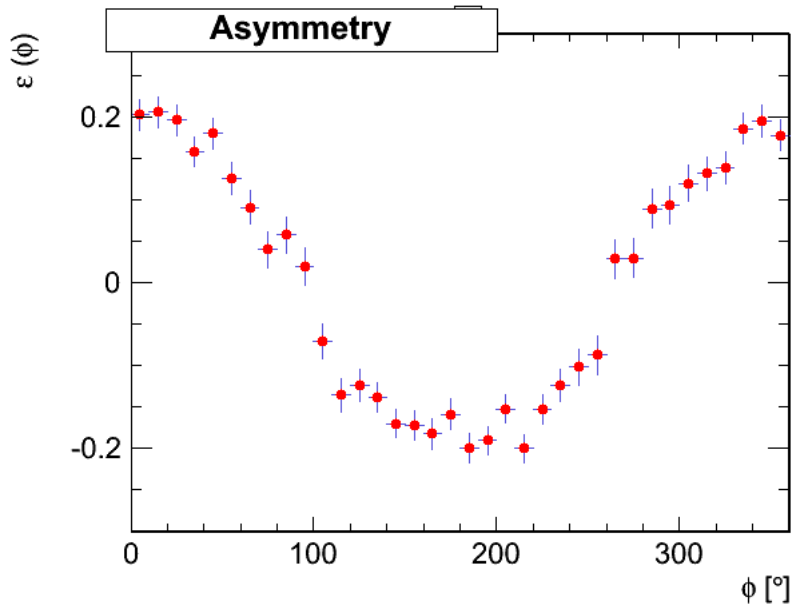

FIGURE 6.14: Asymmetry of reconstructed neutron with respect to azimuthal angle

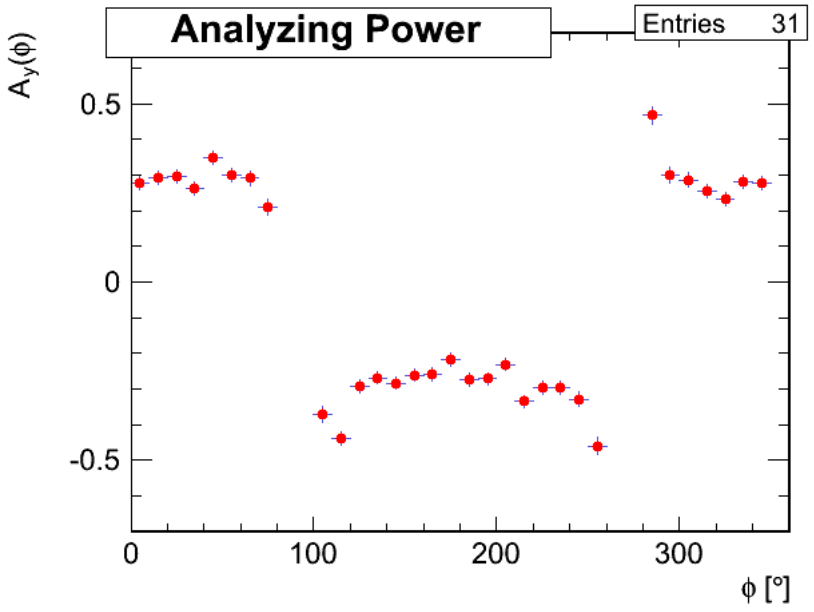

FIGURE 6.15: Breakup analyzing power in the respect to neutron azimuthal angle

6.7.1 Dependence on polar angle

Additionally, analyzing power as the function of neutron polar angle in center of mass system was investigated. First of all, data was selected according to particular range of theta, for instance from 20°to 30°in the center of mass system. For

this data azimuthal angle assymetry was produced and fitted with cosine function. The fitting parameter is assumed to be analyzing power value for the given θ bin. By repeating the same procedure it is possible to recieve analyzing power as the function of polar angle up to 80°in the center of mass system. These results

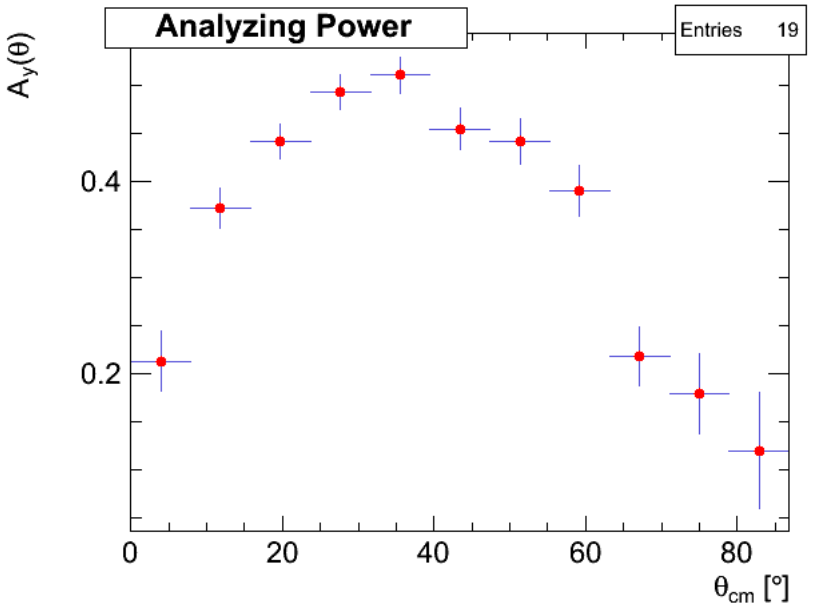

FIGURE 6.16: Breakup analyzing power in the respect to neutron polar angle in c.m.

have potential to put constrains on Chiral Perturbation Theory (χPT) predictions, but the comparison with theory should be performed via sampling method. This method provides opportunity to integrate predictions from a theoretical model of a reaction with three bodies in the final state over the region of phase space covered by given experiment. And only after this procedure is finalized the resuls can be compared, and corresponding conclusions made.

Chapter 7

Results and Discussion

As the first stage of my thesis preparation I have studied the identification of particles, detected by Silicon Tracking Telescopes. These particles are produced by the proton beam, with kinetic energy of 49.3 MeV, hitting the deuterium target at ANKE section.

I have developed codes in order to separate elastic scattering and deuteron break-up events, that provide full kinematic information. Also a code for the polarization measurement, using the double ratio method for proton deuteron elastic scattering was developed.

The result of my analysis of the measurement was that during storing duration of 5000 seconds in the COSY ring the beam polarization decreases from 74.63% to 73.11%. This corresponds to a polarization lifetime of $2.5 \cdot 10^5$ seconds. For optimum conditions, spin-filtering is performed for around two beam lifetimes, in case of the experiments at COSY ring, it was 12000s and 16000s. Based on this fact, the measured polarization lifetime is high enough, and one can conclude that depolarization effects do not influence polarization build-up at COSY significantly and can be ignored.

The other part of my work includes the analysis of break-up events. Since, polarization of the beam was already measured at the first stage of the work, it was possible to deduce the analyzing power for deuteron breakup. The fact that

deuteron breakup is a three body final state reaction adds both interest and difficulty to the problem. Unlike elastic scattering the the analyzing power is not only a function of the polar angle and the cosine of the azimuthal angle, but is function of 5 independent kinematic variables. Experimental dependences of analyzing power as function of polar (up to 80°in the center of mass system) and azimuthal angle (full coverage up to 360°) were gained. However, a comparison with theoretical models and the interpretation of these results are still under development. It requires usage of the so-called sampling method, a multidimensional interpolation to bring theoretical predictions to the form, to be comparable to the experimental results. This comparison should test the validity of current models of three nucleon forces at not yet explored energy regime.

Despite the fact that the proton is a fundamental component of ordinary matter, and one of the most commonplace and stable particles in existence, the proton structure is not yet fully understood. It will be not complete without a direct measurement of transversity. A comprehensive understanding of the proton, as well as of more complicated systems, where three nucleon forces are included, implies an understanding of the strong force, one of the four fundamental forces in nature and the foundation for all of nuclear physics.

Appendix A

Assymetry Statistical Error

The statistical error associated with a measurement of the assymetry $\varepsilon(\theta)$ is given by means of geometrical means δL and δR errors

$$\delta\varepsilon = \sqrt{\left(\frac{\partial\varepsilon}{\partial L}\delta L\right)^2 + \left(\frac{\partial\varepsilon}{\partial R}\delta R\right)^2} =$$
$$= \sqrt{\left(\frac{2R}{(L+R)^2}\delta L\right)^2 + \left(\frac{2L}{(L+R)^2}\delta R\right)^2} =$$
$$= \frac{2}{(L+R)^2}\sqrt{R^2\delta L^2 + L^2\delta R^2} =$$

$$= \frac{1}{L+R}\sqrt{\left(\frac{2R}{L+R}\right)^2(\delta L)^2 + \left(\frac{2L}{L+R}\right)^2(\delta R)^2} =$$
$$= \frac{1}{L+R}\sqrt{\left(1-\frac{L-R}{L+R}\right)^2(\delta L)^2 + \left(1+\frac{L-R}{L+R}\right)^2(\delta R)^2} =$$
$$= \frac{1}{L+R}\sqrt{(1-\varepsilon)^2(\delta L)^2 + (1+\varepsilon)^2(\delta R)^2}$$

For a single counting interval statistical errors are $\delta L = \sqrt{L}$ and $\delta R = \sqrt{R}$, hence expression of statistical error reduces to

$$\delta\varepsilon = \frac{2}{(L+R)^2}\sqrt{R^2L + L^2R} = \sqrt{\frac{4RL(L+R)}{(L+R)^4}} =$$
$$= \sqrt{\frac{4RL}{(L+R)^3}} =$$
$$= \sqrt{\frac{1}{L+R}}\sqrt{(\frac{(L+R)^2 + (L-R)^2}{(L+R)^2})} =$$
$$= \sqrt{\frac{1}{L+R}}\sqrt{(1 - \left(\frac{L-R}{L+R}\right)^2)} =$$
$$= \sqrt{\frac{1-\varepsilon^2}{L+R}}$$

Appendix B

Polarization Calculation Software

Makefile	The makefile for compilation of the PDSelector.cc code
SelectPd.C	The C script that executes PDSelector file for different runs. It provides easy choice of runs, that will be analyzed. One can choose to calculate polarization for only one run, all available runs or some selection of runs.
ElasticKinematicPD	Class from Dynamic Library, developed by Gogi Macharashvili,which describes proton deuteron elastic scattering kinematics, where detector properties are also considered. In the following analyzing code it is used to apply cuts to identify the type of particle in the detector, as well as determining whether particles are stopped in the detector or not

PDSelector.cc	Takes as input root files of tracks.(run number).root format and includes analysis, necessary for particle identification coming form elastic scattering. Gives PDSelectorhisto.root file as output, which includes various distributions of identified elastic particles, we are interested in.
Polarization.C	The main purpose of this code is to calculate the polarization. It take as input file PDSelectorhisto.root, and using distribution of polar angles in different telescopes for different holding fields, calculation of assymetry is performed. Moreover, taking the average value of θ and cosϕ and using analyzing power fitted with 5th order polynom function, the calculation of polarization is held.

Extract from the PDSelector.cc code file.

```
ClassImp(PD_Selector)
PD_Selector::PD_Selector(const char * name, Double_t Pbeam)
: Selector(name, Pbeam)
{ Lab_beam.SetPxPyPzE(0,0, sqrt(Pbeam*(2*MassProton + Pbeam)),
(MassProton + Pbeam));
  Lab_target.SetPxPyPzE(0,0,0,MassDeuteron);
  W_Lab = Lab_beam + Lab_target;
  Beta =  - W_Lab.BoostVector();
  pdElastic = new ElasticKinematicsPD(0.0493) ; }

  bool deutron_3_stop = GetPID_3 (E1,E2,E3) >37;
  bool deutron_2_stop = GetPID(E1,E2) >7;
  bool Have_Deutron = deutron_3_stop||deutron_2_stop;
```

```
if (Have_Deutron)
       {  hTkin_Theta->Fill(theta, T_kin);
 p_Deutron3.SetVect(P);
     p_Deutron3.SetE(MassDeuteron + T_kin);
     TLorentzVector Missing = W_Lab -  p_Deutron3;
     double miss_d3 = Missing.M();
     h_missing_from_deutron->Fill(miss_d3);
     hTheta_Deutron->Fill(theta);
 if (BeamPolID == 1)      //Beam Polarization Up
       {   if (Tel == 0)  {
 h_Theta_L1->Fill(theta);}//Particles scattered to the left
         else      {
h_Theta_R2->Fill(theta);//Particles scattered to the right }
       }
 else if (BeamPolID == 0)   //Beam Polarization Down
     {
     if (Tel == 0)
       {
 h_Theta_R1->Fill(theta);//Particles scattered to the right
       }
     else
       {
 h_Theta_L2->Fill(theta);///Particles scattered to the left
       }
   }
```

Extract from the code about reconstructing deuterons from protons, identified as coming form elastic scattering

```
bool proton_stop = GetPID_3 (E1,E2,E3) >20 && GetPID_3 (E1,E2,E3) <30 &&
(T_kin -  TkinPTheor)>-0.001 && (T_kin -  TkinPTheor)<0.0015;
```

```
if (proton_stop)
       {   hTkin_Theta->Fill(theta, T_kin);
       h_Dif->Fill(T_kin -  TkinPTheor);
       TVector3 protonMom = Track->P() ;
       Proton.SetVectM(protonMom,MassProton);
       Proton_CM = Proton;
       Proton_CM.Boost(Beta);
       Deuteron_CM.SetVectM(-Proton_CM.Vect(),MassDeuteron);
       Deuteron =  Deuteron_CM;
       Deuteron.Boost(-Beta);
       TVector3 Deuteron_Mom =Deuteron.Vect();
       double theta_deu= Deuteron.Theta()*TMath::RadToDeg();
     if (BeamPolID == 1)      //Beam Polarization Up
   {    if (Tel == 1) {
h_Theta_L1->Fill(theta_deu);//Protons are scattered to the right,
//reconstructed deuterons are added to the count on the left
         }
        else {
h_Theta_R2->Fill(theta_deu);//Protons are scattered to the left,
//reconstructed deuterons are added to the count on the right
         }
      }
 if (BeamPolID == 0)//Beam Polarization Down
   { if (Tel == 1){
 h_Theta_R1->Fill(theta_deu);//Protons are scattered to the left,
// reconstructed deuterons are added to the count on the right
         }
        else
         {
 h_Theta_L2->Fill(theta_deu);}}//Protons are scattered to the right,
// reconstructed deuterons are added to the count on the left
```

Appendix C

Analyzing Power data for pd elastic scattering at 49.3 MeV

θ_{cm}	θ_{lab}	$A_{y_{cm}}$	$A_{y_{lab}}$
12.5091017130027	80.4882666387929	0.123	0.002
15.0148804103121	78.5944114781378	0.133	0.001
17.5153544321611	76.7108435608798	0.145	0.002
20.0185415309917	74.8325739361458	0.154	0.002
22.5191253792488	72.9646564847763	0.158	0.002
27.5248001948703	69.2549698636728	0.187	0.002
35.032303829228	63.78125400712	0.162	0.003
40.0355131015573	60.2062182922191	0.118	0.003
43.8589379187419	57.5199319302865	0.07	0.004
47.4744671706031	55.0201042072495	0.015	0.004
51.1518201757407	52.5213016755664	-0.035	0.004
54.8996894603417	50.0235525773558	-0.116	0.007
58.7358138962356	47.5218748370021	-0.213	0.007
60.0448667014542	46.6815554079177	-0.238	0.005
62.656393806534	45.0262871910263	-0.29	0.008

65.0470780692789	43.5364559119941	-0.345	0.006
66.6987717212316	42.5217931484943	-0.369	0.006
70.0465872256223	40.502998106718	-0.43	0.006
70.8547965433082	40.0233883964724	-0.446	0.018
75.0459509681308	37.5859834394969	-0.504	0.007
77.5542932967328	36.1679582783305	-0.515	0.007
80.0916390875355	34.7652428436395	-0.517	0.009
82.5861098448661	33.4177425420209	-0.507	0.009
85.0448567678314	32.1204264480656	-0.524	0.010
90.047072635515	29.5764576817214	-0.492	0.009
95.1072596577128	27.1331709390487	-0.376	0.010
100.008182693884	24.890086417998	-0.249	0.009
105.069747508689	22.6975006199304	-0.06	0.009
107.59001861267	21.6512539138445	0.057	0.021
110.05828996544	20.6549511973272	0.078	0.013
112.596706166958	19.658763631956	0.143	0.018
115.076620583483	18.712487881207	0.148	0.010
120.109641218987	16.8700110782279	0.176	0.009
124.988414366559	15.1772172221547	0.198	0.009
130.126871543937	13.4846779320755	0.151	0.010
135.048820866899	11.9416801084597	0.144	0.009
140.032279275496	10.4486180208179	0.095	0.008
145.055230998377	9.0054578068529	0.09	0.008
160.076495412024	4.97510590648624	0.05	0.009

Appendix D

Breakup Analysis Software

Makefile	The makefile for compilation of the PPNSelector.cc code
SelectPPN.C	The C script that executes PPNSelector file for different runs. It provides easy choice of runs, that will be analyzed. One can choose to calculate polarization for only one run, all available runs or some selection of runs.
PPNSelector.cc	Takes as input root files of tracks.(run number).root format and includes analysis, necessary for particle identification coming from deuteron breakup reaction. Gives PPNSelectorhisto.root file as output, which includes various distributions of identified protons and reconstructed neutron, coming from breakup. Of particular interest are angle distributions of reconstructed neutron, that are used in the following analysis

PhiAssymetry.C	The main purpose of this code is to calculate the assymetry according to neutron azimuthal angle It take as input file PPNSelectorhisto.root, and using distributions of azimuthal angles for different holding fields, calculation of assymetry is performed. Moreover, analyzing powers ad funcitons azimuthal and polar angles are scrutinized.

Extract from the PhiAssymetry.C code file. 1. Getting histograms from PPNSelectorhisto.root

```
TH1F* h_Phi_Up_all= (TH1F*)gDirectory->Get("h_Phi_Up_all");
 TH1F* h_Phi_Down_all= (TH1F*)gDirectory->Get("h_Phi_Down_all");
h_Phi_Up_all->Sumw2();
```

2. Considering luminosity ratio for beam polarization “up” and beam polarization “down“

```
  h_Phi_Down_all->Scale(1.19);//0.798046);
```

3. Asymmetry Calculation

```
TH1F*  h_Sum_all = (TH1F*)h_Phi_Up_all->Clone("h_Phi_Up_all");
  TH1F*  h_Difference_all= (TH1F*) h_Phi_Up_all->Clone("h_Phi_Up_all");
 h_Sum_all-> Add(h_Phi_Down_all);
  h_Difference_all-> Add(h_Phi_Down_all, -1);

  h_Asymmetry_all = (TH1F*)h_Difference_all->Clone("h_Difference_all");
  h_Asymmetry_all-> Divide( h_Sum_all);
```

D.1 Analyzing power dependence on polar angle

1. Calculating asymmetry by the same principle, but considering neutron θ_{cm} 10°slices of data.

```
 for(int d = 0 ; d < 19 ; d++)
    {
      TString name = "h_Phi_Up" ;
      name += d ;
      h_Phi_Up[d] = (TH1F*)gDirectory->Get(name);
      h_Phi_Up[d]->Sumw2();
TString name_down = "h_Phi_Down" ;
      name_down += d ;
      h_Phi_Down[d] = (TH1F*)gDirectory->Get(name_down);  }
```

2. Extracting Analyzing power as fitting parameter of cosine for each 10°bin data set.

```
 for(int d = 0 ; d < 19 ; d++)
    {
      h_Analyzing_Power[d]->Fit(fit_COS[d]);
      Analyzing_Power=  fit_COS[d] ->GetParameter(2);
      Analyzing_Power_Error= fit_COS[d]->GetParError(2);
      h_Parameters->SetBinContent(d,Analyzing_Power);
      h_Parameters->SetBinError(d,Analyzing_Power_Erro);
}
```

Bibliography

[1] Adler et. al. *Phys. Rev. Lett.*, 93:202002, Nov 2004. URL http://link.aps.org/doi/10.1103/PhysRevLett.93.202002.

[2] C. Montag F.Rathman, B.Braun D.Fick, and W.Haeberli G.Graw. New method to polarize protons in a storage ring and implications to polarize antiprotons. *Physical Review Letters*, 71(9):1379–1382, August 1993. URL http://prl.aps.org/abstract/PRL/v71/i9/p1379_1.

[3] Frank Rathmann for PAX Collobaration Paolo Lenisa. Summary of the August to October 2011 PAX beam-time at COSY. pages 1–8, October 2011. URL http://www2.fz-juelich.de/ikp/pax/portal/documents/proposals/files/beamrequest20110318.pdf.

[4] Pia Thörngren Engblom for PAX Collobaration. Measurement of spin observables in pd breakup reaction. pages 1–43, September 2009. URL http://www2.fz-juelich.de/ikp/pax/portal/documents/proposals/files/loi20090727_updated.pdf.

[5] H.-O. Meyer T.J.Whitaker H.Witala J.Golak H. Kamada A. Nogga J.Kuros-Zolnierczuk, P. Thörngren Engblom and R. Skibinski. Faddev calculations of breakup reactions with realistic experimental constraints. *Few-Body System*, 34:259–273, May 2004. URL http://www.springerlink.com/content/ec70930f16x7ya5a/.

[6] J. I. Friedman M. Breidenbach, D. H. Coward H. DeStaebler J. Drees L. W. Mo H. W. Kendall, E. D. Bloom, and R. E. Taylor. Observed behavior of highly inelastic electron-proton scattering. *Physics Letter B*, 23:935–939,

October 1969. URL http://link.aps.org/doi/10.1103/PhysRevLett.23.935.

[7] J. Ashman et all. A measurement of the spin asymmetry and determination of the structure function g1 in deep inelastic muon-proton scattering. *Physics Letters B*, 206(2):364 – 370, 1988. ISSN 0370-2693. doi: 10.1016/0370-2693(88)91523-7. URL http://www.sciencedirect.com/science/article/pii/0370269388915237.

[8] J. Ashman et all. An Investigation of the Spin Structure of the Proton in Deep Inelastic Scattering of Polarized Muons on Polarized Protons. *NuclealPhysics*, B328:1, 1989. doi: 10.1016/0550-3213(89)90089-8.

[9] C.F.Perdrisat and V.Punjabi. The JLab polarization transfer measurements of proton elastic form factor. *Pramana*, 61(5):827–835, November 2002. URL http://www.springerlink.com/content/a7k35384mm738711/.

[10] J. D. Bjorken. Asymptotic sum rules at infinite momentum. *Physical Review*, 179(Issue 5):1547–1553, October 1969. URL http://prola.aps.org/abstract/PR/v179/i5/p1547_1.

[11] W. Tung. Bjorken scaling. *Scholarpedia*, 4(3), 2009. URL http://www.scholarpedia.org/article/Bjorken_scaling.

[12] C. G. R. Callan and D. J. Gross. High-energy electroproduction and the constitution of the electric current. *Physical Review Letters*, 22:156–159, 1969. URL http://link.aps.org/doi/10.1103/PhysRevLett.22.156.

[13] R.P. Feynman. Very high-energy collisions of hadrons. *Physical Review Letters*, 23:1415–1417, 1969. URL http://prl.aps.org/abstract/PRL/v23/i24/p1415_1.

[14] D. E. Soper J. C. Collins and G. Sterman. Factorization for short distance hadron-hadron scattering. *Nuclear Physics B*, 261:104, 1985. URL http://www.sciencedirect.com/science/article/pii/0550321385905656.

[15] D. E. Soper J. C. Collins and G. Sterman. Soft gluons and factorization. *833*, 308, 1988.

[16] George Sterman J.C. Collins, E. Soper. Transverse momentum distribution in Drell-Yan pair and W and Z boson production. *Nuclear Physics B*, 179: 199–224, 1985. URL http://www.sciencedirect.com/science/article/pii/0550321385904791.

[17] J.Soffer. Positivity constraints for spin dependent parton distributions. *Physical Review Letters*, pages 1292–1294. URL http://arxiv.org/pdf/hep-ph/9409254.pdf.

[18] D. Oellers et al. Polarizing a stored proton beam by spin flip? *Physics Letter B*, 674(Issue4-5):269–275, April 2009. URL http://www.sciencedirect.com/science/article/pii/S0370269309003268.

[19] C.Barschel. Calibration of the Breit-Rabi polarimeter for the PAX spin-filtering experiment at COSY/Jülich and AD/CERN. *Diploma Thesis*, Cologne University, 2011.

[20] Ch.Weidemann. Preparations for the spin-filtering experiments at COSY/Jülich. *Thesis, (PhD)*, Cologne University, 2011.

[21] Gerald G. Ohlsen and Jr. P. W. Keaton. Techniques for measurement of spin 1/2 and spin 1 polarization analyzing tensors. *Nuclear Instruments and Methods*, 109(8):41 –59, January 1973. URL http://www.sciencedirect.com/science/article/pii/0029554X73904503.

[22] G. Macharashvili. The software development for the silicon detector data analysis at ANKE-COSY. *PAX Technotes*, pages 1–42, August 2010. URL http://apps.fz-juelich.de/pax/paxwiki/images/6/6c/TechNote15.pdf.

[23] J.L. Romero N.S.P.King, R.M. Larimer Ullmann, H.E.Conzett, and R.Roy. Polarization in proton-deuteron scattering at 50 mev. *Physics Letters*, 69B (2):151–153, August 1977. URL http://www.sciencedirect.com/science/article/pii/0370269377906311.

[24] S.Bertelli. Proton induced deuteron breakup reaction studies at COSY. *Thesis, (PhD)*, Ferrara University, 2011.